X-765-73-25
PREPRINT

NASA TM X- 66169

EFFECTS OF PROTON IRRADIATION AND TEMPERATURE ON 1Ω-CM AND 10Ω-CM SILICON SOLAR CELLS

Omega

C. NICOLETTA

JANUARY 1973

GSFC — GODDARD SPACE FLIGHT CENTER —
GREENBELT, MARYLAND

41 p

X-765-73-25

EFFECTS OF PROTON IRRADIATION AND TEMPERATURE ON 1Ω-cm AND 10Ω-cm SILICON SOLAR CELLS

C. Nicoletta

January 1973

GODDARD SPACE FLIGHT CENTER
Greenbelt, Maryland

EFFECTS OF PROTON IRRADIATION AND TEMPERATURE ON 1Ω-cm AND 10Ω-cm SILICON SOLAR CELLS

C. Nicoletta

ABSTRACT

1Ω-cm and 10Ω-cm Silicon Solar cells, manufactured by AEG-Telefunken, were exposed to 1.0 Mev protons at a fixed flux of 10^9 P/cm^2-sec and fluences of 10^{10}, 10^{11}, 10^{12} and 3.10^{12} P/cm^2. I-V curves of the cells were made at room temperature, -65°C and +165°C after each irradiation. A value of 139.5 mw/cm^2 was taken as AMO incident energy rate per unit area. Degradation occurred for both uncovered 1Ω-cm and 10Ω-cm cells. Efficiencies are generally higher than those of comparable U.S. cells tested earlier. Damage (loss in maximum power efficiency) with proton fluence is somewhat higher for 10Ω-cm cells, measured at the three temperatures, for fluences above 2.10^{11} P/cm^2. Cell efficiency, as expected, changes drastically with temperature.

CONTENTS

	Page
GENERAL INTRODUCTION	1
THEORETICAL BACKGROUND	1
EXPERIMENTAL TECHNIQUE	4
RESULTS	5
CONCLUSIONS	7
ACKNOWLEDGMENT	7
REFERENCES	8

TABLES

Table		Page
1	Experiment 1 — 1Ω-cm	9
2	Experiment 2 — 10Ω-cm	10
3	Experiment 3 — 10Ω-cm (200μ)	11
4	Experiment 4 — 1Ω-cm 50% Covered	12
5	Experiment 5 — 10Ω-cm 50% Covered	13
6	Comparison of Relative Power Output from Data in Statler's Paper with that from GSFC	14

EFFECTS OF PROTON IRRADIATION AND TEMPERATURE ON 1Ω-cm AND 10Ω-cm SILICON SOLAR CELLS

GENERAL INTRODUCTION

1Ω-cm and 10Ω-cm solar cells, manufactured by AEG-Telefunken of West Germany for use on the Helios satellite, have recently been exposed to 1.0 Mev proton radiation. Past data indicates maximum degradation of cell efficiency for unshielded solar cells at roughly (1.0-1.5) Mev (Ref. 1). Fluence levels have been selected to coincide with those used in earlier radiation experiments on U.S. manufactured cells (Refs. 2 and 3). Fluences of 10^{10}, 10^{11}, 10^{12} and 3.10^{12} P/cm^2 were attained in each experiment at a flux of 10^9 P/cm^2-sec.

The cells were irradiated at room temperature and I-V characteristics measured at that temperature and at the two extremes likely to be found in the mission, -65°C and +165°C.

The cells are then compared as to their efficiencies, taken from the I-V curves.

THEORETICAL BACKGROUND

Low energy proton (E < 2.0 Mev) irradiation of uncovered silicon solar cells affects the junction properties of silicon enough to produce large power losses (Ref. 2). The penetration of 1.0 Mev protons in silicon is a function of energy only and is shown in Figure 1. This curve has been obtained from Linnenbom's data (Ref. 4) for aluminum, using the equation,

$$\frac{R_{Si}}{R_{Al}} = \frac{\left(\frac{dE}{dr}\right)_{Al}}{\left(\frac{dE}{dr}\right)_{Si}} \qquad (1)$$

the R's are the ranges and the (dE/dr)'s the stopping powers. The relative mass stopping power of Al to Si is 0.97. From Figure 1, 1.0 Mev protons can be seen to penetrate about 16μ into silicon. This value is well below the p-n junction, which is generally about .25-.50 micron below the surface. Larger proton fluences cause increased defects to be produced in the semiconductor, thereby creating more trapping sites and decreasing efficiency of the cell overall. From the expression for diffusion length of minority carriers, $L = (D\tau)^{1/2}$, where D is

the diffusion constant and τ the carrier lifetime, as the lifetime decreases due to increased trapping sites, so does the diffusion length. This directly affects the short circuit current, measured in the experiments, through the expression,

$$I_{SC} = A\,q\,(L_e + L_h)\,G \tag{2}$$

where A is the exposed cell area, q the electron charge, L_e and L_h the diffusion lengths of electrons and holes respectively, and G the rate of production of (e - h) pairs. Looking at the results in the text, Figures 4-15, before irradiation and after a fluence of 3.10^{12} P/cm^2, one observes the degradation of short circuit current.

The current-voltage characteristic of the p-n junction is denoted by the diode equation,

$$I = I_0 \left(e^{\frac{qV}{kT}} - 1\right) \tag{3}$$

where I is the injection current flowing through the junction under a forward bias voltage, V. k is Boltzman's Constant and T is the absolute temperature. I_0 is the saturation current due to free carriers which overcome the junction barrier potential, and is exponentially temperature dependent. In the laboratory measurements of the I-V curves, where a finite load is used, the net current through the load is the difference between the short circuit current and injection current,

$$I_{net} = I_{sc} - I_0 \left(e^{\frac{qV}{kT}} - 1\right) \tag{4}$$

When $I_{net} = 0$, we get the open circuit voltage, V_{oc},

$$V_{oc} = \frac{kT}{q} \ln \left(\frac{I_{sc}}{I_0} + 1\right) \tag{5}$$

Since our primary concern is with maximum power output and cell efficiency, we would like an expression which relates the three observed values of current, voltage and temperature.

By definition, power output P(V) is,

$$P(V) = V I_{net} = V I_{sc} - V I_0 \left(e^{\frac{qV}{kT}} - 1\right) \tag{6}$$

Maximum power occurs at $\partial P / \partial V = 0$, therefore from Equation (6) we get,

$$I_{sc} = \left(V_{mp} \frac{q}{kT} + 1\right) I_0 e^{\frac{qV_{mp}}{kT}} - I_0 \tag{7}$$

where V_{mp} is the voltage at maximum power. The net current at maximum power is

$$I_{mp} = I_{sc} - I_0 \left(e^{\frac{qV_{mp}}{kT}} - 1\right) \tag{8}$$

Substituting Equation (7) into Equation (8), we get

$$I_{mp} = I_0 \frac{q}{kT} V_{mp} e^{\frac{qV_{mp}}{kT}} \tag{9}$$

From the definition of maximum power, $V_{mp} I_{mp}$, we have

$$P_{mp} = I_0 \frac{q}{kT} V_{mp}^2 e^{\frac{qV_{mp}}{kT}} \tag{10}$$

Elimination of the exponential term in (10) gives

$$P_{mp} = \frac{I_{sc} \frac{q}{kT} V_{mp}^2}{\left(1 + \frac{q}{kT} V_{mp}\right)} \left(1 + \frac{I_0}{I_{sc}}\right) \tag{11}$$

Solar cell efficiency, η, is maximum power output/power input

$$\eta = \frac{I_{sc} \frac{q}{kT} V_{mp}^2 \left(1 + \frac{I_0}{I_{sc}}\right)}{\left(1 + \frac{q}{kT} V_{mp}\right) A\,(\text{AMO S.C.})} \tag{12}$$

(see Ref. 5), where (AMO S.C.) is the air mass zero solar constant. The efficiency represents the single most important quantity representing the solar cell's function in power conversion. In our case, due to low energy (< 2 Mev) proton irradiation, it has more significance in describing damage to the cell than damage coefficients, since the 1.0 Mev protons do not pass through the cell. One cannot directly therefore relate the damage coefficient to diffusion lengths.

From Expression (12) we can see that the efficiency decreases with increasing temperature. Greater fluences account for decreases in minority carrier lifetimes, thereby decreasing the short circuit current.

EXPERIMENTAL TECHNIQUE

Four (2 × 2) cm cells are irradiated simultaneously in a turbo-molecular pumped vacuum chamber. The vacuum was approximately 10^{-6} torr throughout the irradiations and measurements. Figure 2 is an illustration of the experimental set-up. Each solar cell had four leads; two on the buss bar and two on the Ti (Pd) Ag layer on the back of the cell, to reduce resistance loss.

The proton beam was supplied by a Van de Graaff accelerator with energy stability of ±1.0%. The proton beam flux was measured over the sample positions by five Faraday cups. One cup was centered over each sample in the experiment, (4 samples) and the fifth was centrally located. Variation in the proton flux was found to be about 50% over the four samples. The samples were fastened to a copper sample holder, using silver epoxy, in all experiments except the first one. In the first experiment the samples were spring loaded to the sample holder, but due to contact problems (see Ref. 6), the silver epoxy cement was subsequently used to achieve good contact.

The sample temperatures were maintained by circulating gaseous nitrogen for the low temperatures, and using electric ceramic heaters for the high temperatures. A copper-constantan thermocouple on the copper substrate monitored

substrate temperature and is the value assumed for cell temperatures. Due to nitrogen circulation problems, it was difficult to maintain a constant -65°C for all measurements.

A Spectrolab X-25 solar simulator with a 3000 watt filtered Xe lamp was used in making the I-V measurements. A value of 139.5 mw/cm^2 was maintained as AMO during all measurements. The variation of the light beam over the samples was determined by moving the turning mirror (Figure 2) to strike one sample at different positions. The variation was found to be ±2.0%. A Spectrolab D550 electronic load coupled to an x-y plotter provided the I-V curves on metric paper. The temperature of the four cells was brought from room temperature to -65°C then up to +165°C after each proton fluence was reached. The proton flux was maintained within experimental limitations at 10^9 P/cm^2-sec.

Five experiments were performed in all. Each consisted of three uncovered solar cells and one covered cell. Four levels of fluence were reached in each experiment; 10^{10}, 10^{11}, 10^{12} and 3.10^{12} P/cm^2. The three uncovered cells in each experiment consisted of:

three 1Ω-cm cells (300μ thick), experiment 1;
three 10Ω-cm cells (300μ thick), experiment 2;
three 10Ω-cm cells (200 μ), experiment 3;
three 1Ω-cm cells 50% covered, experiment 4;
three 10Ω-cm cells 50% covered, experiment 5.

The covered solar cell is shielded by about 150μ of fused silica, thereby preventing the protons from reaching the cell surface. Figure 3 is a plot of proton penetration in fused silica taken from Linnenbom (Ref. 4). In effect then, the covered cells were measured at the three different temperatures, but shielded from the incident radiation by the cover slides.

I-V measurements were started immediately after irradiation to minimize any annealing effects.

RESULTS

Characteristic I-V curves giving cell power output in watts were generated for each measurement. Figures 4-15 show typical I-V curves for the five experiments, before irradiation and after 3.10^{12} P/cm^2. The I-V curves for intermediate fluences are omitted in this report. The I-V curves of the covered solar cells 81-13, Figures 4 and 5, show the results during Experiment 1, which are typical of the results for that cell during the other experiments. No radiation damage is noted.

At room temperature, before irradiation, most of the cells show the same efficiency to within 0.6% for each experiment.

Tables 1-5 give the values of the open circuit voltage and short circuit current with proton fluence and temperature. Note the short circuit current decreases little until after a fluence $> 10^{10}$ Protons/cm^2. The defects introduced by the irradiation are now more significantly affecting the diffusion lengths. This is shown in the plot of diffusion length with fluence for 4.6 Mev protons (Ref. 3). To consider damage coefficients here would be misleading, as discussed earlier, due to the short penetration of 1.0 Mev protons.

Of prime importance in rating a cell is efficiency, the expression for which is given in Equation (12). For the input power we use 139.5 mw/cm^2 supplied by our Solar Simulator. Typical variations in per cent efficiencies with fluence, at three temperatures, are given in Figures 16 thru 21. The efficiencies of the covered cells change very little with fluence, see Figure 16. As predicted by Equation (12), the efficiency is greater for lower temperatures.

The per cent damage versus fluence is given in Figure 22. The results are compared with those in Statler's paper (Ref. 1), which were taken from earlier work.

The ratio of P_{max}/P_{max_0}, maximum power output to maximum power output before irradiation, versus proton energies, with fluences as parameters, is reported in Statler's work. Those results are at room temperature. The approximate results from his paper and our data are compared in Table 6.

The above values are maximum power ratios due to 1.0 Mev protons at room temperature irradiation. The AEG-Telefunken cells exhibit less radiation damage than the previously tested American cells.

Existing published temperature data, other than room temperature, following proton irradiation is scarce, but our results give what we believe to be significant data at the two temperature (-65°C and +165°C) values.

The 1Ω-cm covered cell in each experiment was measured at the three temperatures of 25°C, -65°C and +165°C but was not exposed to radiation. Figure 23 compares the efficiencies, of this cell to a similar uncovered one irradiated to 3×10^{12} P/cm^2, at different temperatures. The difference between the curves would be due to radiation damage. The efficiencies of the covered AEG cells are higher than those of U.S. cells studied at Ames at 28°C and 200°C (Ref. 7).

CONCLUSIONS

(1) The solar cells examined in any particular experiment appear fairly uniform as regards their I-V curves, before irradiation, at room temperature.

(2) 10Ω-cm cells exhibit somewhat greater damage than 1Ω-cm cells, due to proton fluence.

In Cherry and Slifer's work in 1963 (Ref. 8) with 4.6 Mev protons, they found 10Ω-cm cells to be more radiation resistant than 1Ω-cm cells. Use of tungsten light source in obtaining their I-V curves provides a long wavelength response, where the 1Ω-cm cells exhibited greater degradation than the 10Ω-cm cells. Our results, using a Xenon light source, show a response in the short wavelength region and here we found 10Ω-cm to exhibit slightly greater damage.

(3) The amount of damage with proton fluence appears greater for cells measured at +165°C than for those measured at +25°C and -65°C.

(4) The solar cells examined at room temperature degrade to a lesser extent than the 1Ω-cm and 10Ω-cm cells reported on in Statler's work.

(5) The 50% covered 1Ω-cm and 10Ω-cm cells exhibit less degradation with proton fluence than the uncovered cells, except for the 50% covered 10Ω-cm cell at +165°C. This higher rate may be attributed to a contact problem.

(6) From Figure 22, we note that for both uncovered 1Ω-cm and 10Ω-cm cells measured at 25°C and -65°C, the percent damage varies no more than about 7% for these cells at any particular fluence.

(7) The difference in efficiency between an irradiated and unirradiated cell diminishes as the temperature at which the I-V curves are run increases. See Figure 23.

ACKNOWLEDGMENT

Thanks go to Mr. Arthur DuFault of the Facilities Management Section for irradiation of the cells and to Mr. William Gdula of STACO for assembling the apparatus and running I-V curves.

REFERENCES

1. An Evaluation by Solar Simulation of Radiation Damage in Silicon Solar Cells. R. Statler, IEEE Transactions on Electron Devices, Vol. Ed. 14, No. 1, Jan. 1967.

2. Low-Energy Proton Damage to Silicon Solar Cells. E. Stofel and D. Joslin. The Aerospace Corporation, El Segundo, Calif., U.S. Air Force Contract F04701-70-C-0059.

3. Proton Irradiation Study of Pulled and Float-Zone Silicon Solar Cells. R. Tauke and B. Faraday, Proc. of IEEE, Feb. 1967.

4. Range-Energy Relations for Protons and Electrons in Al, Si and $S_i O_2$. V. J. Linnenbom, NRL Report 5828, Sept. 1962.

5. Physics of Semiconductor Devices. S. M. Sze, pp. 643-644, Wiley-Interscience, New York @ 1969.

6. Memorandum to H. Frankel from J. Jellison, L. Slifer and C. Nicoletta. Subject: Interconnect Failure on Helios Solar Cells.

7. Solar Cell Characteristics at High Solar Intensities and Temperatures. P. Lewis and J. Kirkpatrick, 8th IEEE Photovoltaic Specialists Conference, Seattle, Wash., Aug. 1970.

8. Solar Cell Radiation Damage Studies with 1 Mev Electrons and 4.6 Mev Protons. W. Cherry and L. Slifer, May 1963, GSFC X-636-63-110.

Table 1

Experiment 1 — 1Ω-cm

	80-11									86-2								
fluence P/cm^2	V_{oc} mv	I_{sc} ma	T °C	V_{oc} mv	I_{sc} ma	T °C	V_{oc} mv	I_{sc} ma	T °C	V_{oc} mv	I_{sc} ma	T °C	V_{oc} mv	I_{sc} ma	T °C	V_{oc} mv	I_{sc} ma	T °C
0	590	137	25	775	129	-67	300	147	165	595	134	25	770	128	-62	300	146	164
10^{10}	570	128	24	765	115	-66	275	146	163	570	128	24	765	119	-67	280	146	163
10^{11}	550	113	27	745	98	-65	255	139	164	555	119	25	750	107	-62	260	140	165
10^{12}	520	98	27	715	80	-63	240	129	161	505	101	26	715	88	-62	215	123	163
3.10^{12}	495	84	26	710	67	-63	195	110	165	495	95	27	730	80	-67	190	112	165
	86-3									81-13 (6 mil)								
fluence P/cm^2	V_{oc} mv	I_{sc} ma	T °C	V_{oc} mv	I_{sc} ma	T °C	V_{oc} mv	I_{sc} ma	T °C	V_{oc} mv	I_{sc} ma	T °C	V_{oc} mv	I_{sc} ma	T °C	V_{oc} mv	I_{sc} ma	T °C
0	590	136	25	775	130	-66	300	149	165	595	140	25	780	126	-69	310	150	162
10^{10}	570	130	24	765	118	-68	275	148	164	590	140	25	775	128	-64	300	147	164
10^{11}	545	115	27	735	102	-60	255	140	165	600	138	25	775	129	-65	295	148	164
10^{12}	500	92	26	695	76	-62	195	117	166	590	138	26	-	-	-	310	150	161
3.10^{12}	475	85	27	715	69	-67	175	105	165	595	138	25	770	126	-63	300	146	164

Table 2

Experiment 2 — 10Ω-cm

	151-9									151-13								
fluence P/cm^2	V_{oc} mv	I_{sc} ma	T °C	V_{oc} mv	I_{sc} ma	T °C	V_{oc} mv	I_{sc} ma	T °C	V_{oc} mv	I_{sc} ma	T °C	V_{oc} mv	I_{sc} ma	T °C	V_{oc} mv	I_{sc} ma	T °C
0	550	143	25	645	137	-67	225	148	164	555	138	25	650	132	-65	225	143	165
10^{10}	530	143	26	635	134	-62	215	150	165	545	139	26	630	132	-64	225	143	165
10^{11}	490	116	26	635	110	-63	180	133	166	515	127	26	640	120	-63	200	138	165
10^{12}	410	102	25	630	90	-64	140	107	165	480	108	25	630	98	-63	160	116	165
3.10^{12}	470	95	26	630	83	-63	130	90	165	480	102	26	635	89	-63	140	104	164
	151-15									81-13 (6 mil)								
fluence P/cm^2	V_{oc} mv	I_{sc} ma	T °C	V_{oc} mv	I_{sc} ma	T °C	V_{oc} mv	I_{sc} ma	T °C	V_{oc} mv	I_{sc} ma	T °C	V_{oc} mv	I_{sc} ma	T °C	V_{oc} mv	I_{sc} ma	T °C
0	545	138	26	645	131	-66	225	142	165	595	137	26	775	123	-63	300	147	165
10^{10}	530	138	26	615	130	-61	215	140	165	595	138	25	750	126	-64	300	147	165
10^{11}	495	127	26	615	121	-62	200	136	165	595	139	26	750	129	-62	305	147	165
10^{12}	450	108	26	585	93	-63	160	123	165	595	138	26	750	129	-62	300	146	165
3.10^{12}	415	87	26	555	73	-63	120	100	164	595	138	26	755	127	-64	300	150	165

Table 3

Experiment 3 — 10Ω-cm (200μ)

	150-7									150-8								
fluence P/cm^2	V_{oc} mv	I_{sc} ma	T °C	V_{oc} mv	I_{sc} ma	T °C	V_{oc} mv	I_{sc} ma	T °C	V_{oc} mv	I_{sc} ma	T °C	V_{oc} mv	I_{sc} ma	T °C	V_{oc} mv	I_{sc} ma	T °C
0	525	131	26	610	129	-61	205	132	164	525	129	26	600	126	-61	205	130	164
10^{10}	525	131	26	615	124	-62	200	133	165	520	128	26	605	119	-64	195	131	166
10^{11}	500	123	27	610	110	-57	185	130	165	500	123	26	605	109	-57	190	129	165
10^{12}	480	102	24	615	94	-65	150	113	164	450	88	24	590	79	-64	125	102	164
3.10^{12}	490	98	22	600	85	-42	120	98	165	450	81	22	560	68	-42	95	80	165
	150-13									81-13 (6 mil)								
fluence P/cm^2	V_{oc} mv	I_{sc} ma	T °C	V_{oc} mv	I_{sc} ma	T °C	V_{oc} mv	I_{sc} ma	T °C	V_{oc} mv	I_{sc} ma	T °C	V_{oc} mv	I_{sc} ma	T °C	V_{oc} mv	I_{sc} ma	T °C
0	525	132	26	605	130	-61	205	133	164	595	137	25	755	129	-62	305	147	164
10^{10}	525	130	25	605	123	-61	190	134	164	590	139	26	755	127	-64	300	148	165
10^{11}	490	115	27	605	101	-57	170	128	165	590	138	25	740	127	-57	305	147	163
10^{12}	470	96	24	605	88	-62	130	106	164	585	138	25	750	126	-64	300	147	165
3.10^{12}	470	86	21	590	76	-42	105	85	165	585	138	22	750	128	-43	300	148	165

Table 4

Experiment 4 — 1Ω-cm 50% Covered

	81-2									81-1								
fluence P/cm^2	V_{oc} mv	I_{sc} ma	T °C	V_{oc} mv	I_{sc} ma	T °C	V_{oc} mv	I_{sc} ma	T °C	V_{oc} mv	I_{sc} ma	T °C	V_{oc} mv	I_{sc} ma	T °C	V_{oc} mv	I_{sc} ma	T °C
0	600	140	23	765	125	-65	300	146	164	590	140	23	745	128	-65	300	145	164
10^{10}	580	132	25	765	115	-68	290	147	165	585	136	25	760	121	-68	300	145	164
10^{11}	590	126	25	760	113	-65	280	142	165	585	129	25	755	117	-65	280	144	165
10^{12}	540	111	26	750	93	-66	240	130	164	545	117	26	750	100	-66	250	134	165
3.10^{12}	525	105	25	740	89	-65	220	123	165	540	112	25	740	97	-65	230	128	165
	81-3									81-13 (6 mil)								
fluence P/cm^2	V_{oc} mv	I_{sc} ma	T °C	V_{oc} mv	I_{sc} ma	T °C	V_{oc} mv	I_{sc} ma	T °C	V_{oc} mv	I_{sc} ma	T °C	V_{oc} mv	I_{sc} ma	T °C	V_{oc} mv	I_{sc} ma	T °C
0	600	143	23	760	132	-63	300	150	164	590	139	23	765	129	-65	305	147	165
10^{10}	595	140	25	770	125	-66	300	150	165	580	139	25	745	127	-64	305	149	165
10^{11}	595	134	25	760	122	-65	285	147	165	585	138	25	735	128	-64	305	147	165
10^{12}	565	123	25	760	107	-65	260	140	165	570	139	26	715	128	-66	310	150	164
3.10^{12}	555	118	26	750	103	-67	240	134	165	555	139	25	700	128	-65	310	148	164

Table 5

Experiment 5 — 10Ω-cm 50% Covered

	151-1									151-2								
fluence P/cm^2	V_{oc} mv	I_{sc} ma	T °C	V_{oc} mv	I_{sc} ma	T °C	V_{oc} mv	I_{sc} ma	T °C	V_{oc} mv	I_{sc} ma	T °C	V_{oc} mv	I_{sc} ma	T °C	V_{oc} mv	I_{sc} ma	T °C
0	550	134	25	640	127	-66	225	140	165	550	135	23	640	129	-65	220	140	165
10^{10}	554	133	24	640	127	-65	225	139	166	550	132	24	640	126	-65	220	140	163
10^{11}	553	128	25	640	113	-63	200	133	165	540	130	25	640	118	-63	200	133	162
10^{12}	500	111	25	640	100	-62	165	115	163	500	115	24	640	105	-64	115	115	163
3.10^{12}	495	109	25	635	96	-64	160	108	163	500	112	25	630	100	-63	113	107	164
										81-13 (6 mil)								
fluence P/cm^2	V_{oc} mv	I_{sc} ma	T °C	V_{oc} mv	I_{sc} ma	T °C	V_{oc} mv	I_{sc} ma	T °C	V_{oc} mv	I_{sc} ma	T °C	V_{oc} mv	I_{sc} ma	T °C	V_{oc} mv	I_{sc} ma	T °C
0										595	138	24	778	125	-66	305	149	163
10^{10}	No Cell Tested									590	139	25	760	128	-63	302	148	164
10^{11}										594	140	25	776	129	-65	300	147	165
10^{12}										595	138	25	760	128	-63	295	147	165
3.10^{12}										595	137	25	765	127	-64	300	148	164

Table 6

Comparison of Relative Power Output from Data in Statler's Paper with that from GSFC

	1Ω-cm 10^{11} P/cm^2	1Ω-cm 3.10^{11} P/cm^2	10Ω-cm 10^{11} P/cm^2	10Ω-cm 3.10^{11} P/cm^2
Statler's Paper	0.65	0.53	0.68	—
GSFC Results	0.76	0.66	0.70	0.67

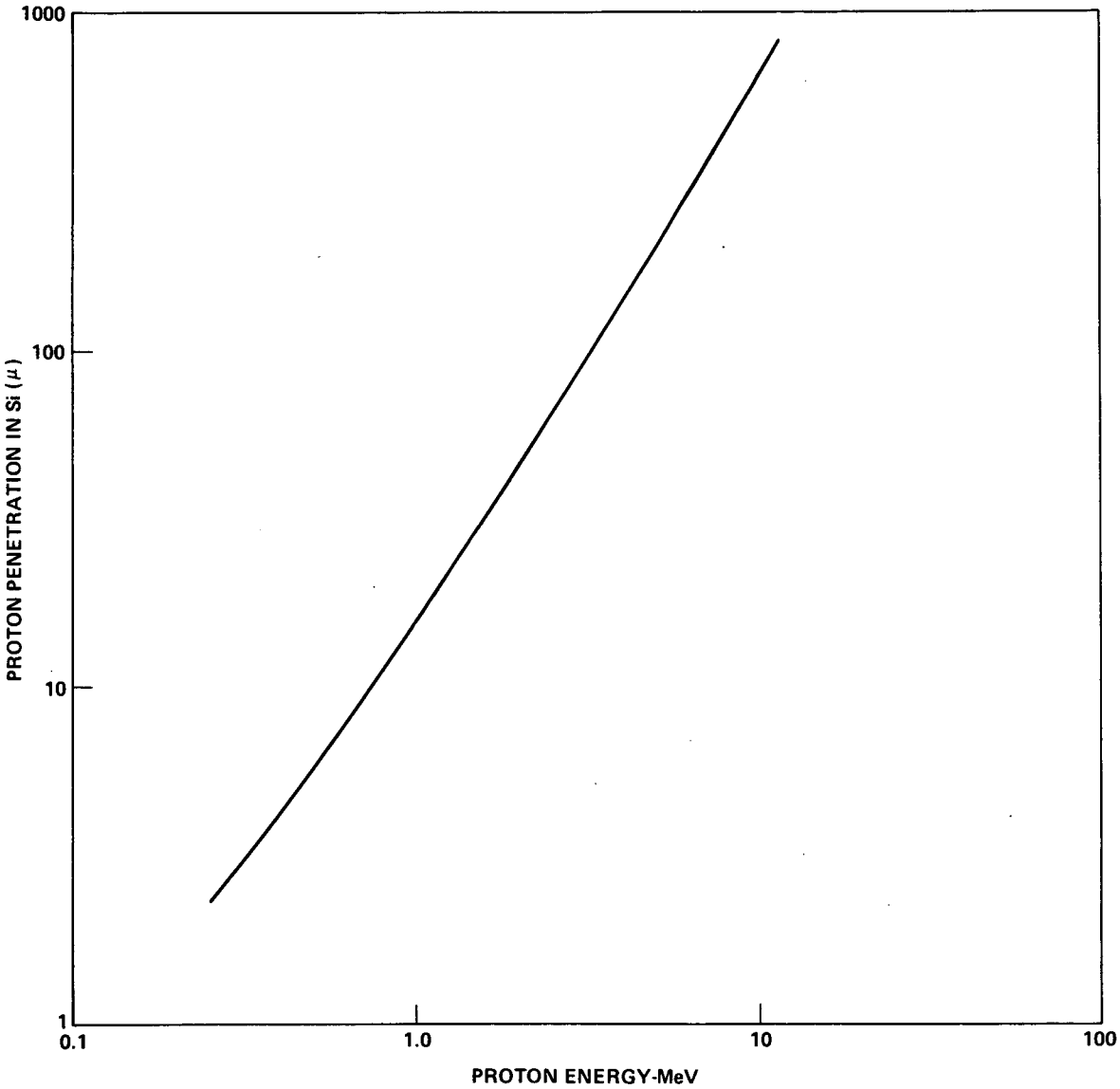
1000
100
10
1
PROTON PENETRATION IN Si (μ)
0.1
1.0
10
100
PROTON ENERGY-MeV

Figure 1

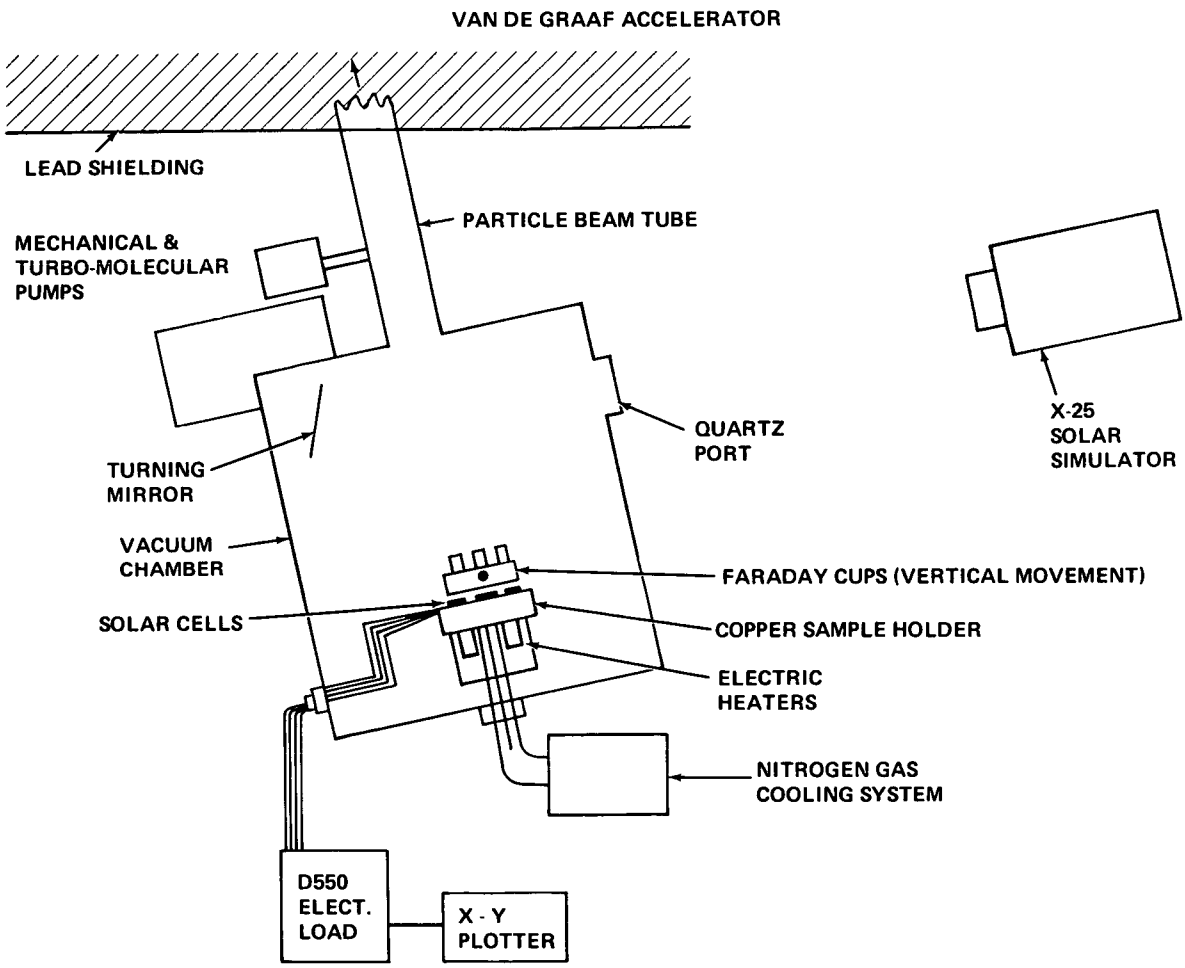

EXPERIMENTAL SET-UP

Figure 2

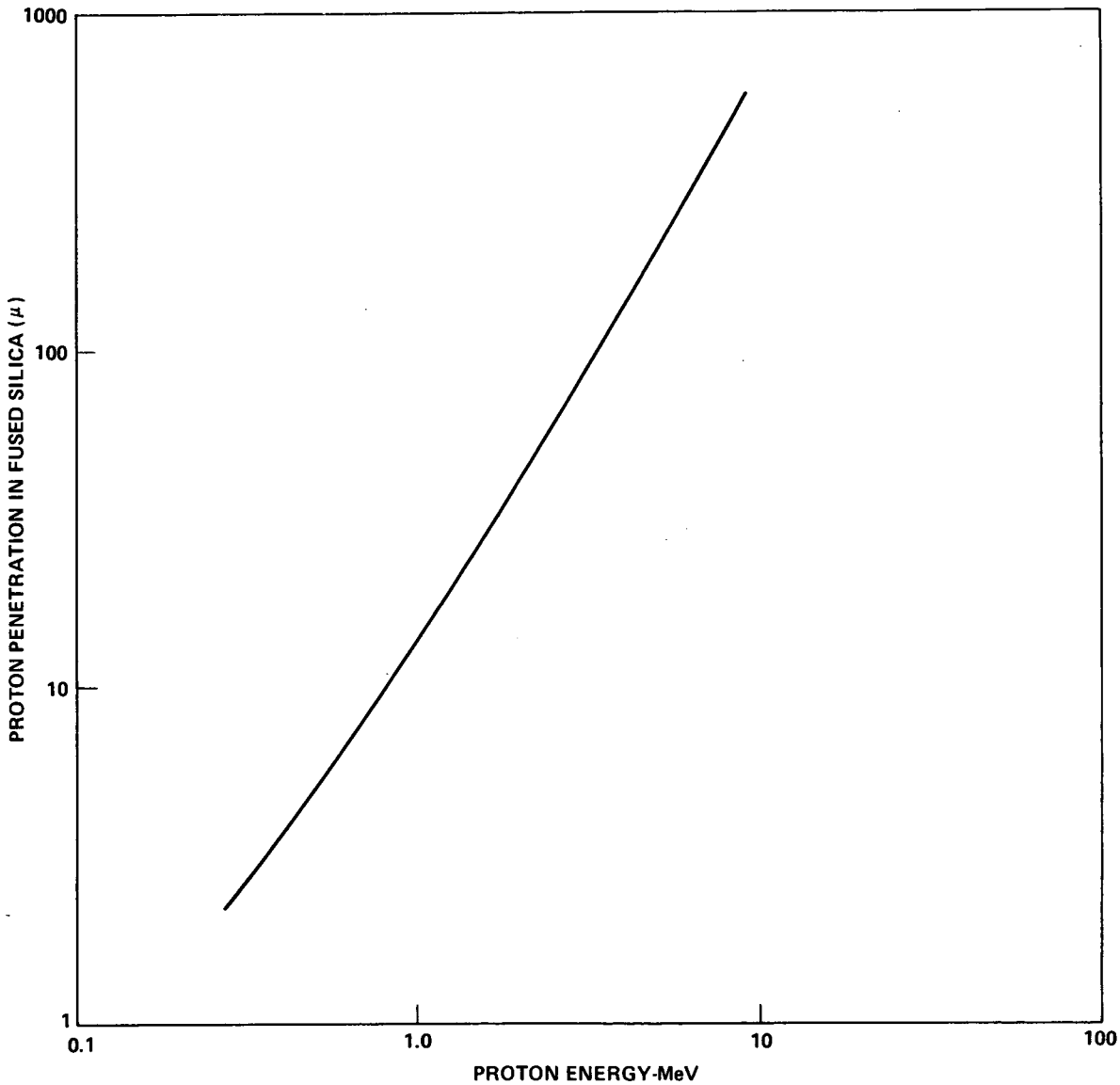
1000
100
10
1
PROTON PENETRATION IN FUSED SILICA (μ)
0.1
1.0
10
100
PROTON ENERGY-MeV

Figure 3

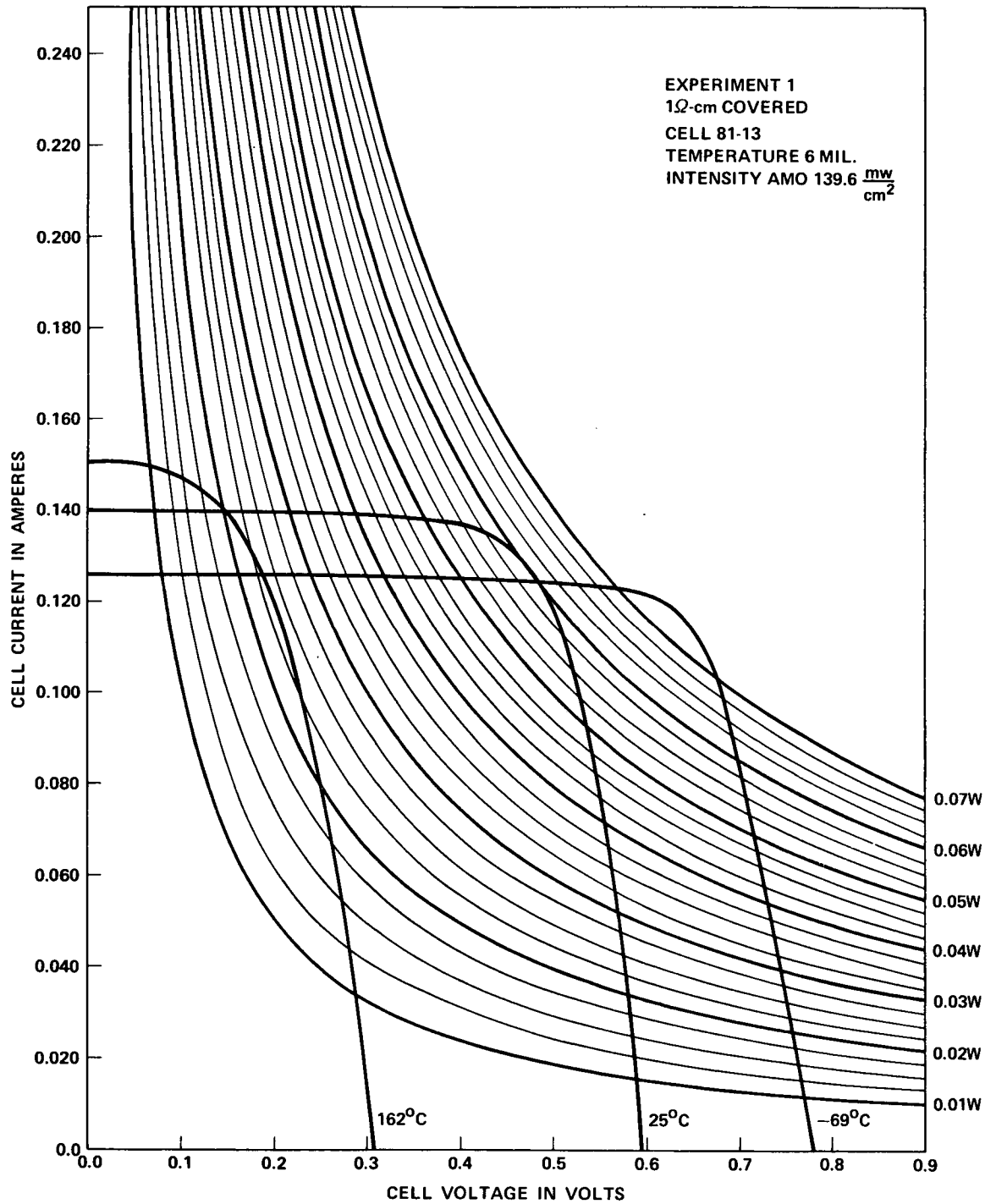
EXPERIMENT 1
1Ω-cm COVERED
CELL 81-13
TEMPERATURE 6 MIL.
INTENSITY AMO 139.6 mw/cm²
CELL CURRENT IN AMPERES
0.240
0.220
0.200
0.180
0.160
0.140
0.120
0.100
0.080
0.060
0.040
0.020
0.0
0.0
0.1
0.2
0.3
0.4
0.5
0.6
0.7
0.8
0.9
CELL VOLTAGE IN VOLTS
0.07W
0.06W
0.05W
0.04W
0.03W
0.02W
0.01W
162°C
25°C
−69°C

Figure 4

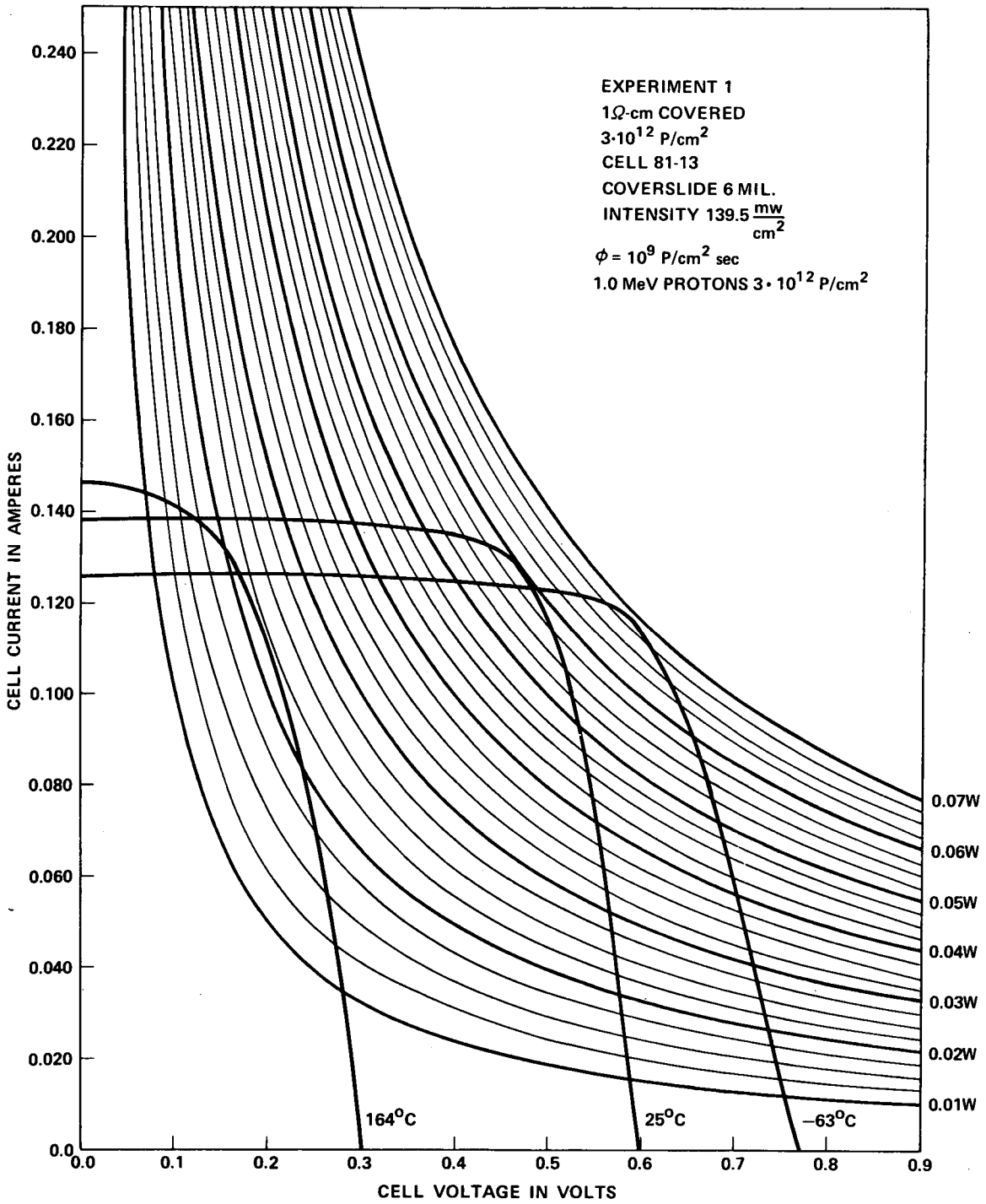
EXPERIMENT 1
1Ω-cm COVERED
3·10^12 P/cm^2
CELL 81-13
COVERSLIDE 6 MIL.
INTENSITY 139.5 mw/cm^2
φ = 10^9 P/cm^2 sec
1.0 MeV PROTONS 3 · 10^12 P/cm^2
CELL CURRENT IN AMPERES
CELL VOLTAGE IN VOLTS
0.240
0.220
0.200
0.180
0.160
0.140
0.120
0.100
0.080
0.060
0.040
0.020
0.0
0.0
0.1
0.2
0.3
0.4
0.5
0.6
0.7
0.8
0.9
0.07W
0.06W
0.05W
0.04W
0.03W
0.02W
0.01W
164°C
25°C
−63°C

Figure 5

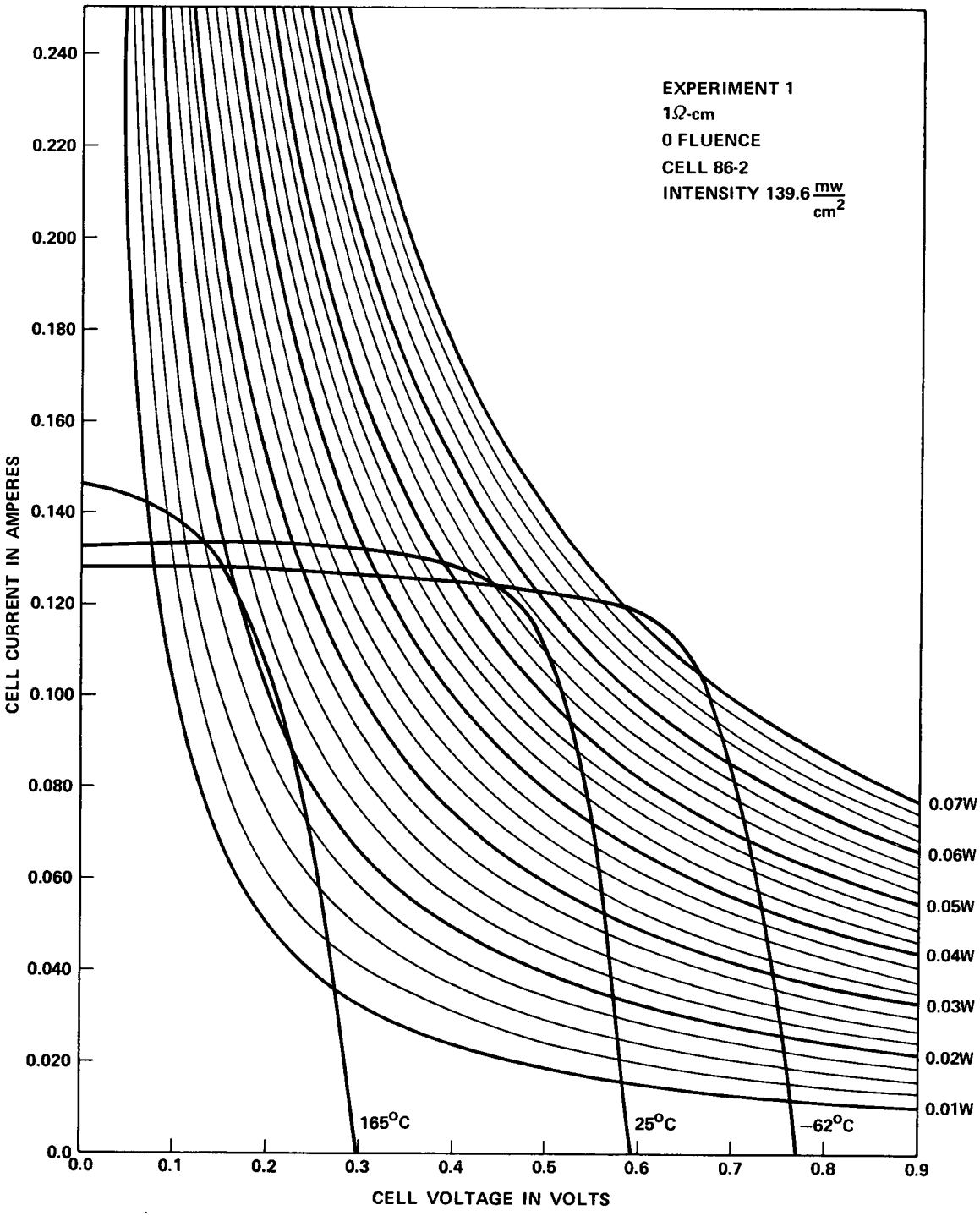
EXPERIMENT 1
1Ω-cm
0 FLUENCE
CELL 86-2
INTENSITY 139.6 mw/cm²
CELL CURRENT IN AMPERES
CELL VOLTAGE IN VOLTS
0.240
0.220
0.200
0.180
0.160
0.140
0.120
0.100
0.080
0.060
0.040
0.020
0.0
0.0
0.1
0.2
0.3
0.4
0.5
0.6
0.7
0.8
0.9
0.07W
0.06W
0.05W
0.04W
0.03W
0.02W
0.01W
165°C
25°C
−62°C

Figure 6

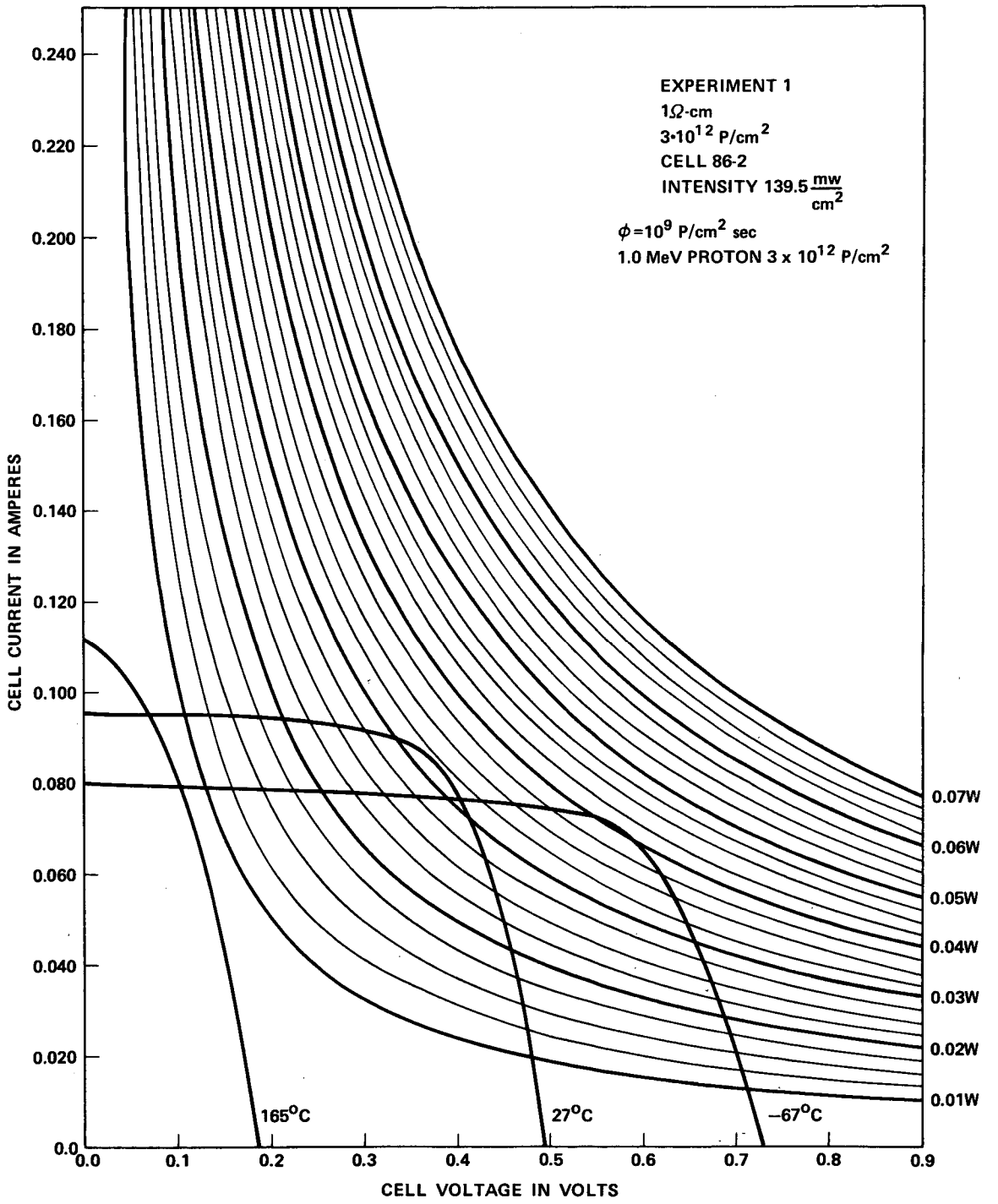
EXPERIMENT 1
1Ω-cm
3•10^12 P/cm^2
CELL 86-2
INTENSITY 139.5 mw/cm^2
φ=10^9 P/cm^2 sec
1.0 MeV PROTON 3 x 10^12 P/cm^2
CELL CURRENT IN AMPERES
CELL VOLTAGE IN VOLTS
0.240
0.220
0.200
0.180
0.160
0.140
0.120
0.100
0.080
0.060
0.040
0.020
0.0
0.0
0.1
0.2
0.3
0.4
0.5
0.6
0.7
0.8
0.9
0.07W
0.06W
0.05W
0.04W
0.03W
0.02W
0.01W
165°C
27°C
-67°C

Figure 7

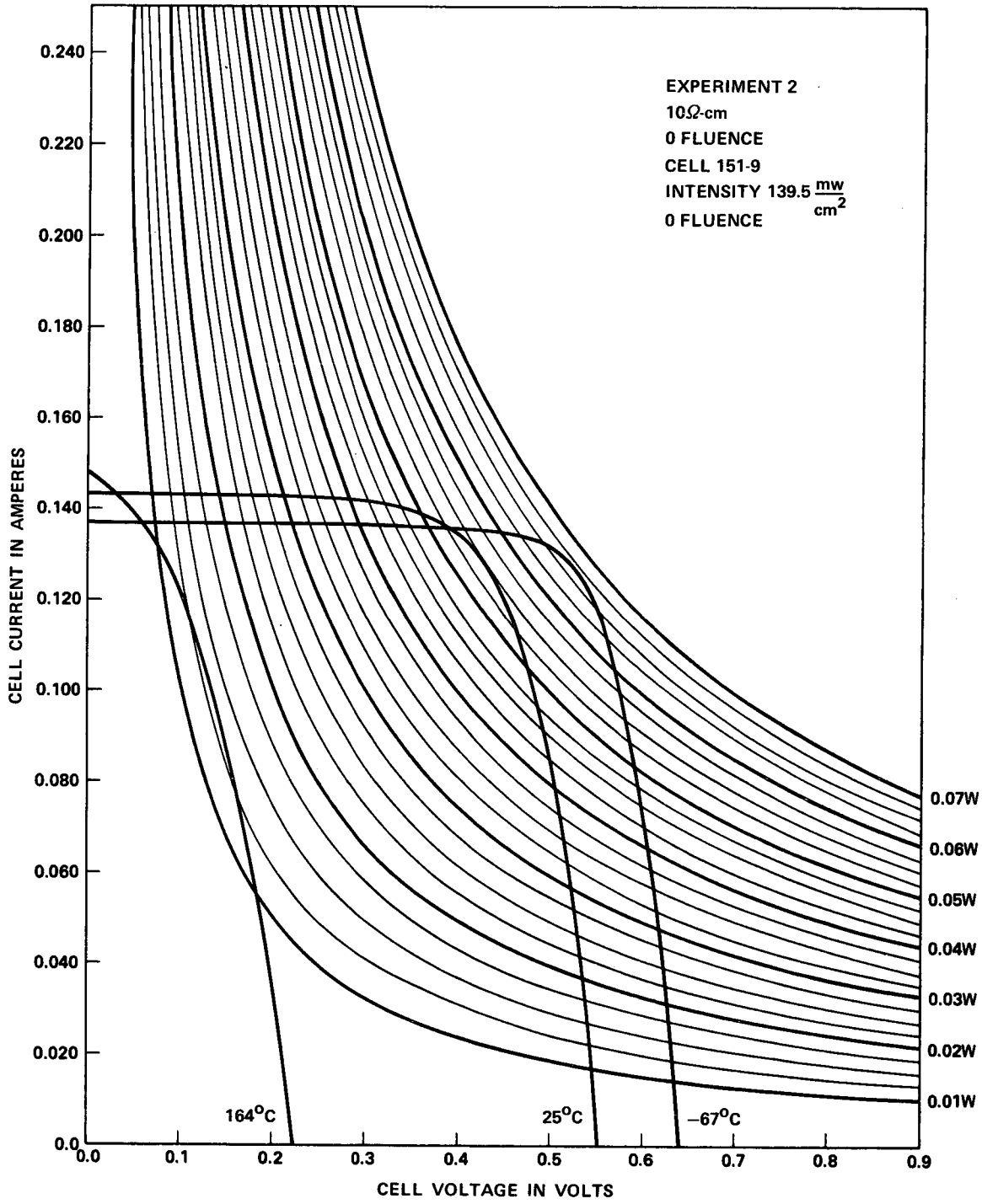
EXPERIMENT 2
10Ω-cm
0 FLUENCE
CELL 151-9
INTENSITY 139.5 mw/cm²
0 FLUENCE
CELL CURRENT IN AMPERES
0.240
0.220
0.200
0.180
0.160
0.140
0.120
0.100
0.080
0.060
0.040
0.020
0.0
0.0
0.1
0.2
0.3
0.4
0.5
0.6
0.7
0.8
0.9
CELL VOLTAGE IN VOLTS
164°C
25°C
−67°C
0.07W
0.06W
0.05W
0.04W
0.03W
0.02W
0.01W

Figure 8

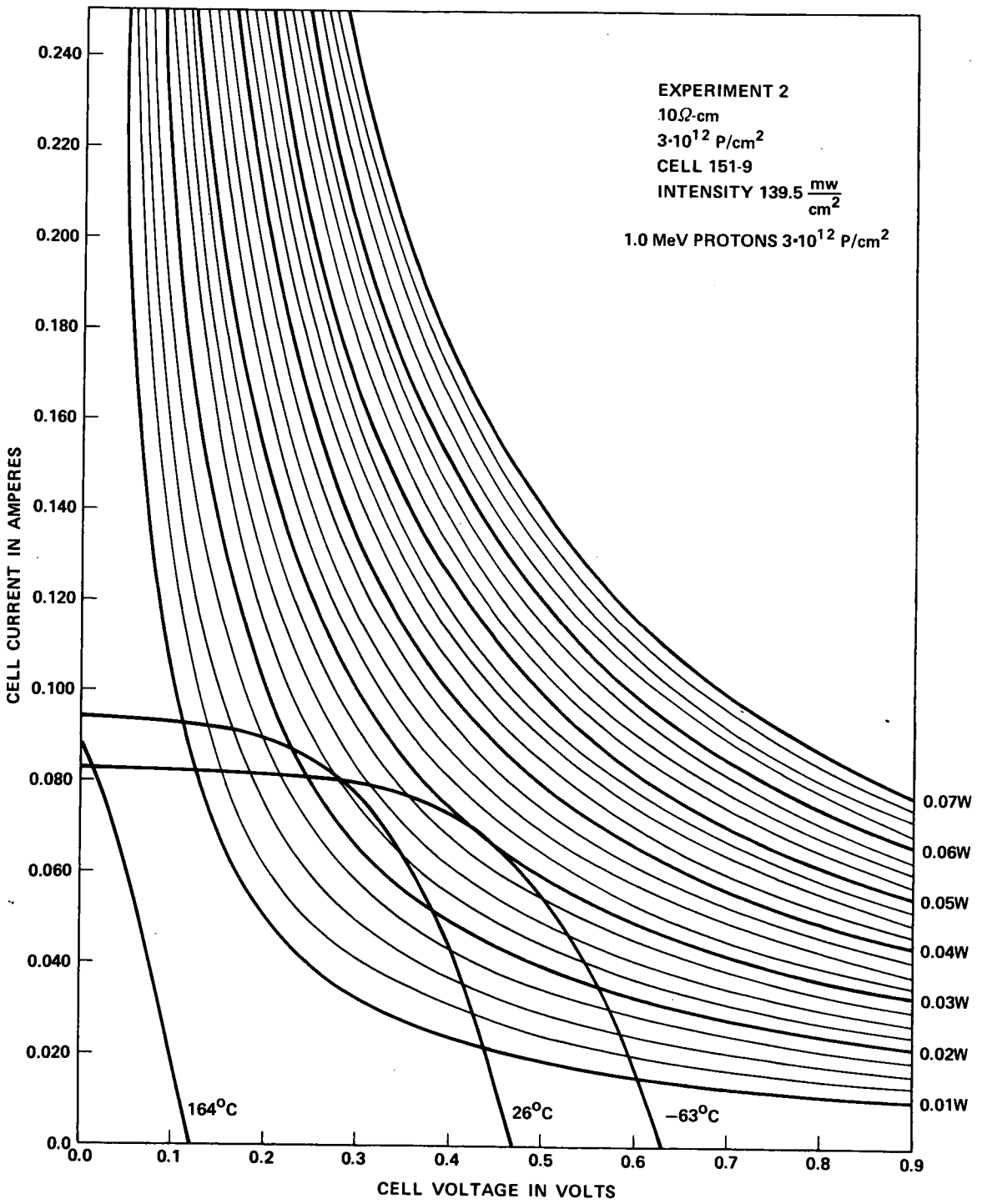
EXPERIMENT 2
10Ω-cm
3·10^12 P/cm^2
CELL 151-9
INTENSITY 139.5 mw/cm^2
1.0 MeV PROTONS 3·10^12 P/cm^2
CELL CURRENT IN AMPERES
CELL VOLTAGE IN VOLTS
0.240
0.220
0.200
0.180
0.160
0.140
0.120
0.100
0.080
0.060
0.040
0.020
0.0
0.0
0.1
0.2
0.3
0.4
0.5
0.6
0.7
0.8
0.9
0.07W
0.06W
0.05W
0.04W
0.03W
0.02W
0.01W
164°C
26°C
−63°C

Figure 9

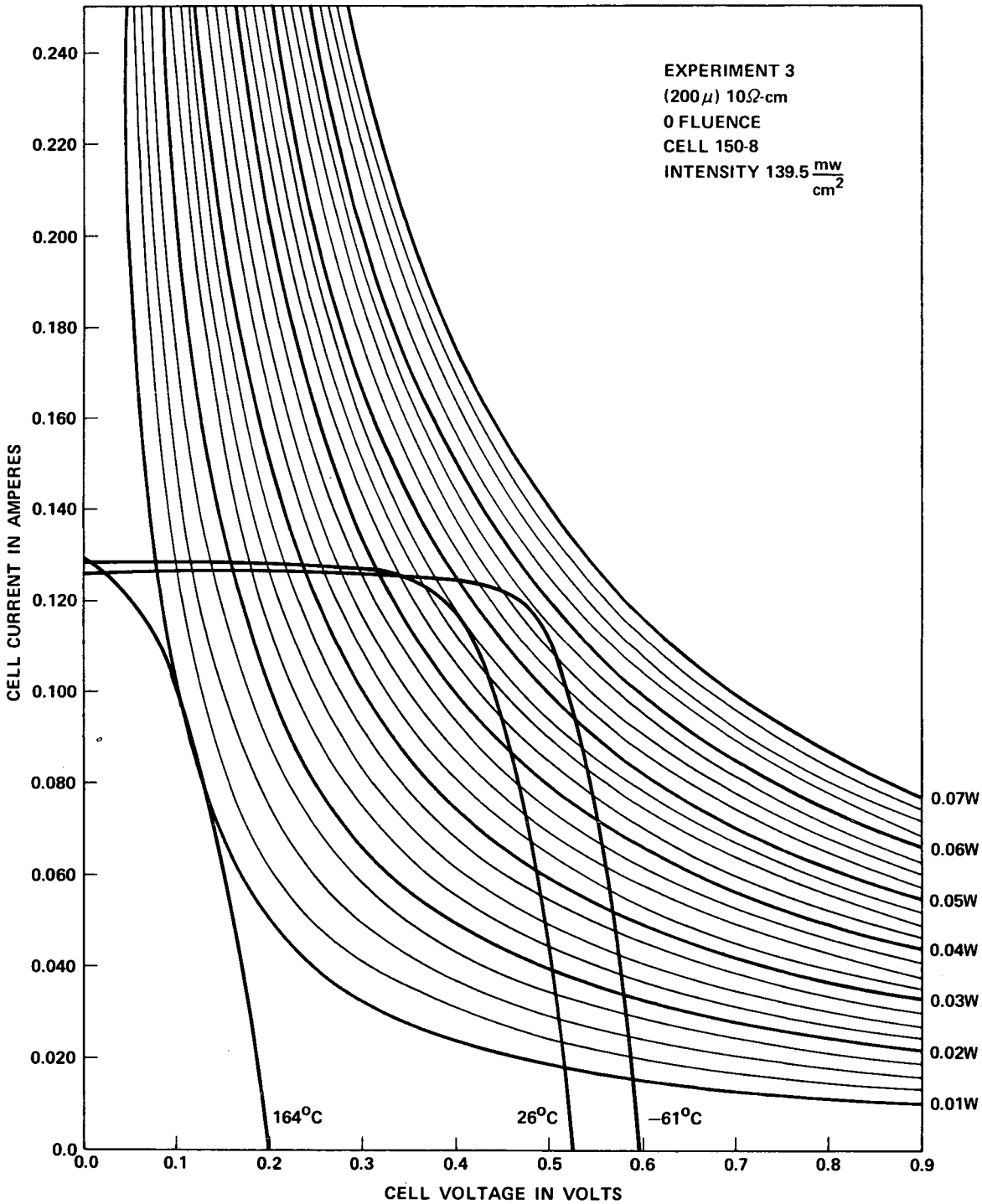
EXPERIMENT 3
(200μ) 10Ω-cm
0 FLUENCE
CELL 150-8
INTENSITY 139.5 mw/cm²
CELL CURRENT IN AMPERES
0.240
0.220
0.200
0.180
0.160
0.140
0.120
0.100
0.080
0.060
0.040
0.020
0.0
0.0
0.1
0.2
0.3
0.4
0.5
0.6
0.7
0.8
0.9
CELL VOLTAGE IN VOLTS
0.07W
0.06W
0.05W
0.04W
0.03W
0.02W
0.01W
164°C
26°C
−61°C

Figure 10

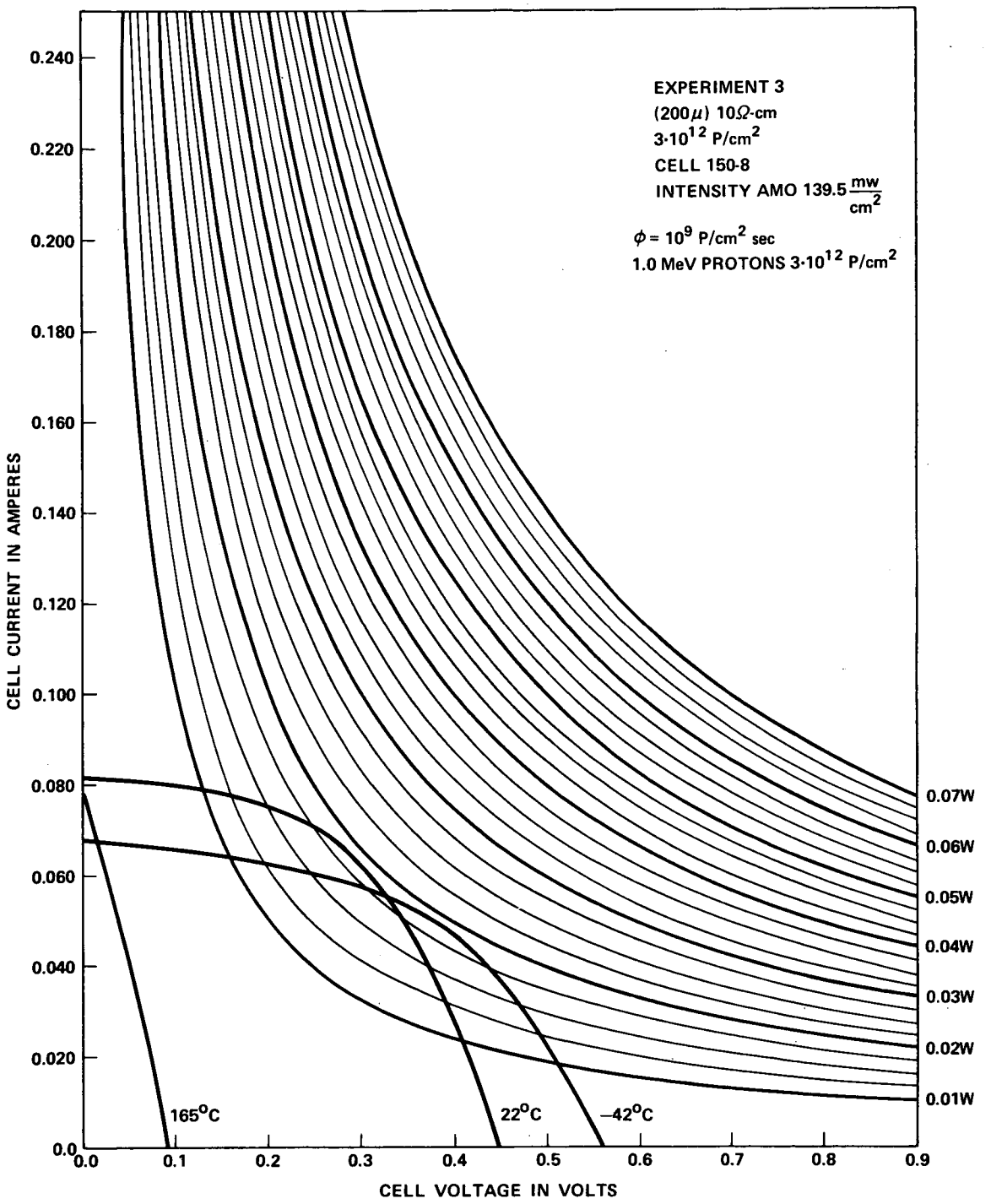
EXPERIMENT 3
(200μ) 10Ω-cm
3·10^12 P/cm^2
CELL 150-8
INTENSITY AMO 139.5 mw/cm^2
φ = 10^9 P/cm^2 sec
1.0 MeV PROTONS 3·10^12 P/cm^2
CELL CURRENT IN AMPERES
CELL VOLTAGE IN VOLTS
0.240
0.220
0.200
0.180
0.160
0.140
0.120
0.100
0.080
0.060
0.040
0.020
0.0
0.0
0.1
0.2
0.3
0.4
0.5
0.6
0.7
0.8
0.9
0.07W
0.06W
0.05W
0.04W
0.03W
0.02W
0.01W
165°C
22°C
−42°C

Figure 11

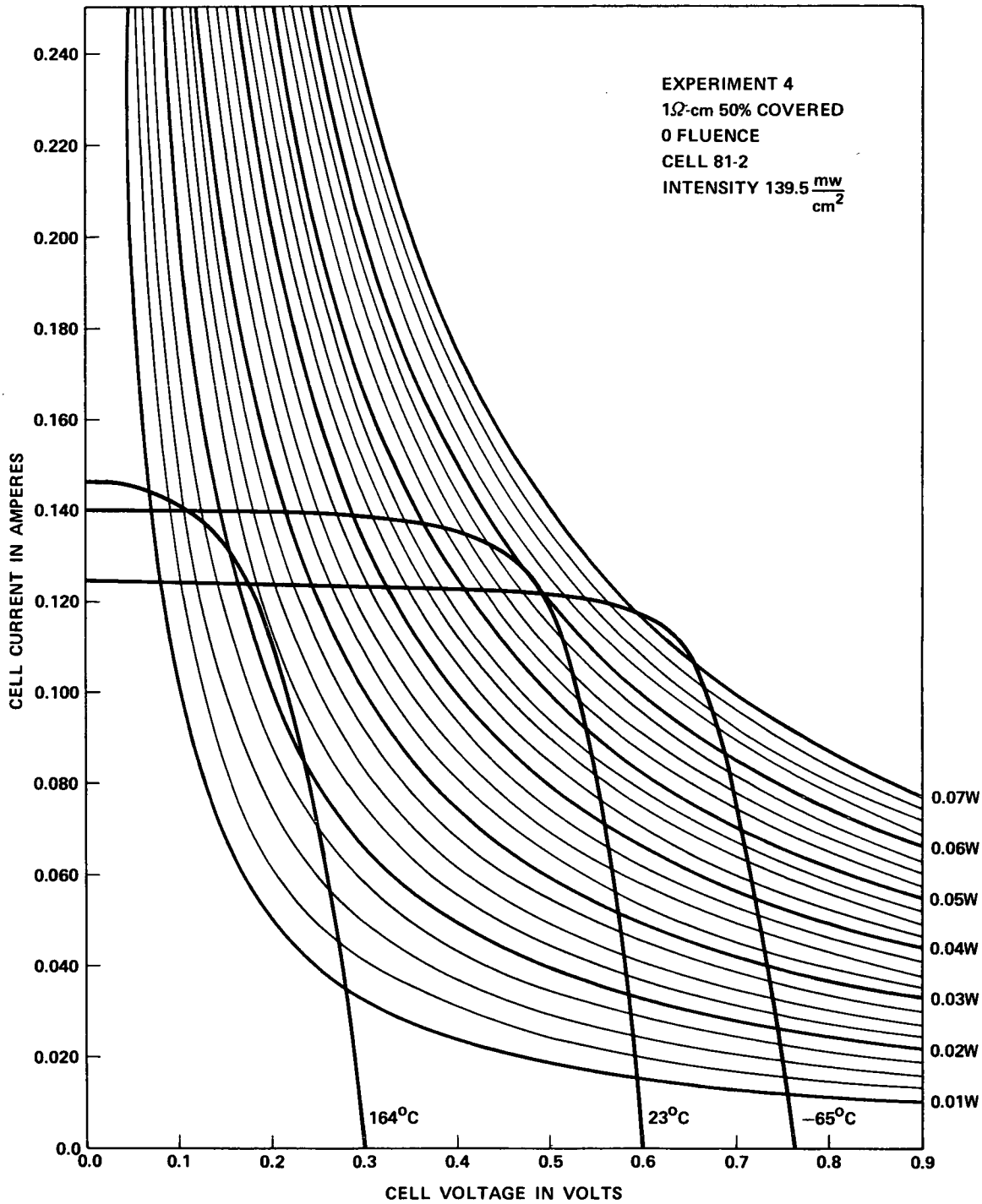
EXPERIMENT 4
1Ω-cm 50% COVERED
0 FLUENCE
CELL 81-2
INTENSITY 139.5 mw/cm²
CELL CURRENT IN AMPERES
CELL VOLTAGE IN VOLTS
0.240
0.220
0.200
0.180
0.160
0.140
0.120
0.100
0.080
0.060
0.040
0.020
0.0
0.0
0.1
0.2
0.3
0.4
0.5
0.6
0.7
0.8
0.9
0.07W
0.06W
0.05W
0.04W
0.03W
0.02W
0.01W
164°C
23°C
−65°C

Figure 12

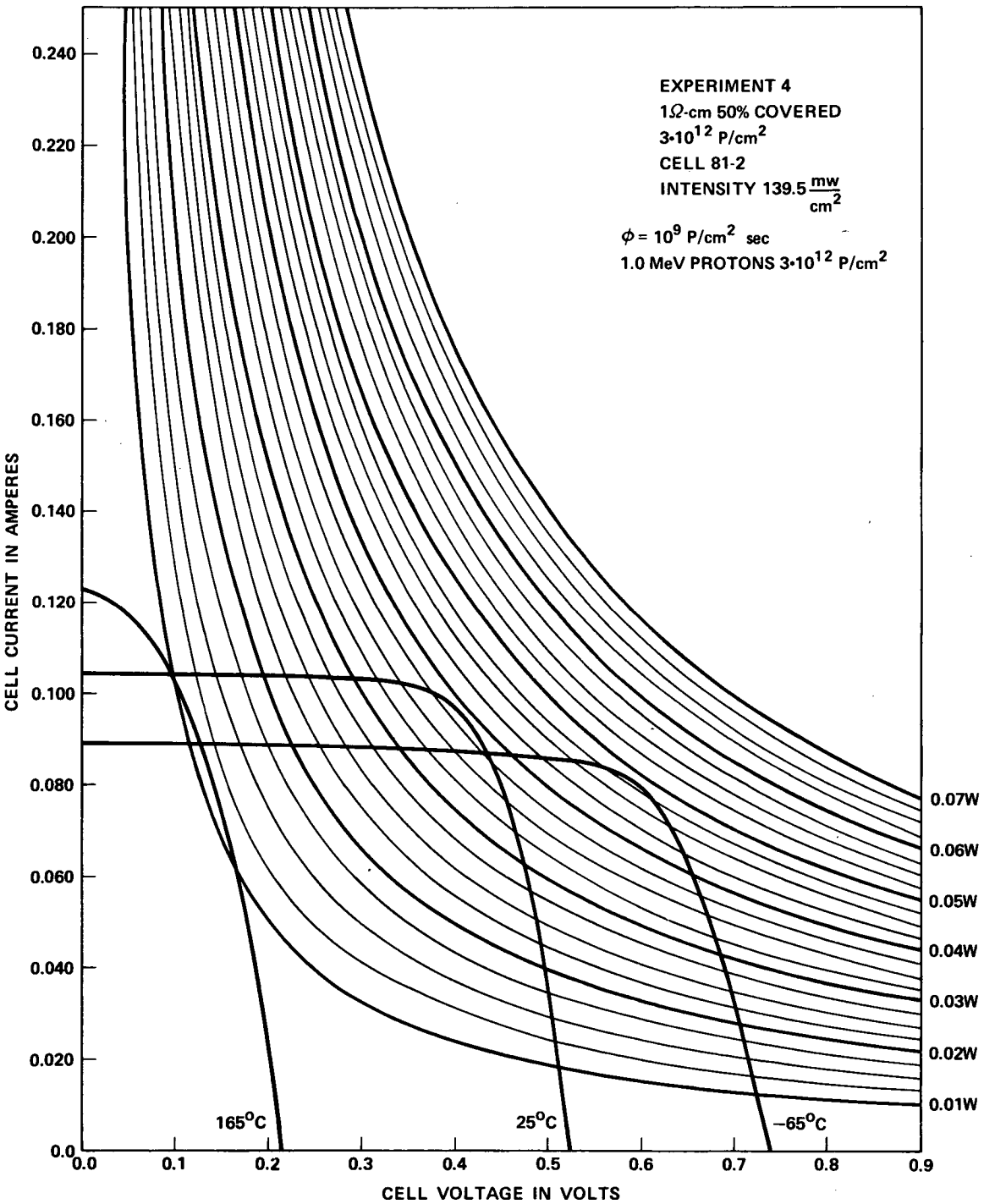
EXPERIMENT 4
1Ω-cm 50% COVERED
3•10^12 P/cm^2
CELL 81-2
INTENSITY 139.5 mw/cm^2
φ = 10^9 P/cm^2 sec
1.0 MeV PROTONS 3•10^12 P/cm^2
CELL CURRENT IN AMPERES
CELL VOLTAGE IN VOLTS
0.240
0.220
0.200
0.180
0.160
0.140
0.120
0.100
0.080
0.060
0.040
0.020
0.0
0.0
0.1
0.2
0.3
0.4
0.5
0.6
0.7
0.8
0.9
0.07W
0.06W
0.05W
0.04W
0.03W
0.02W
0.01W
165°C
25°C
−65°C

Figure 13

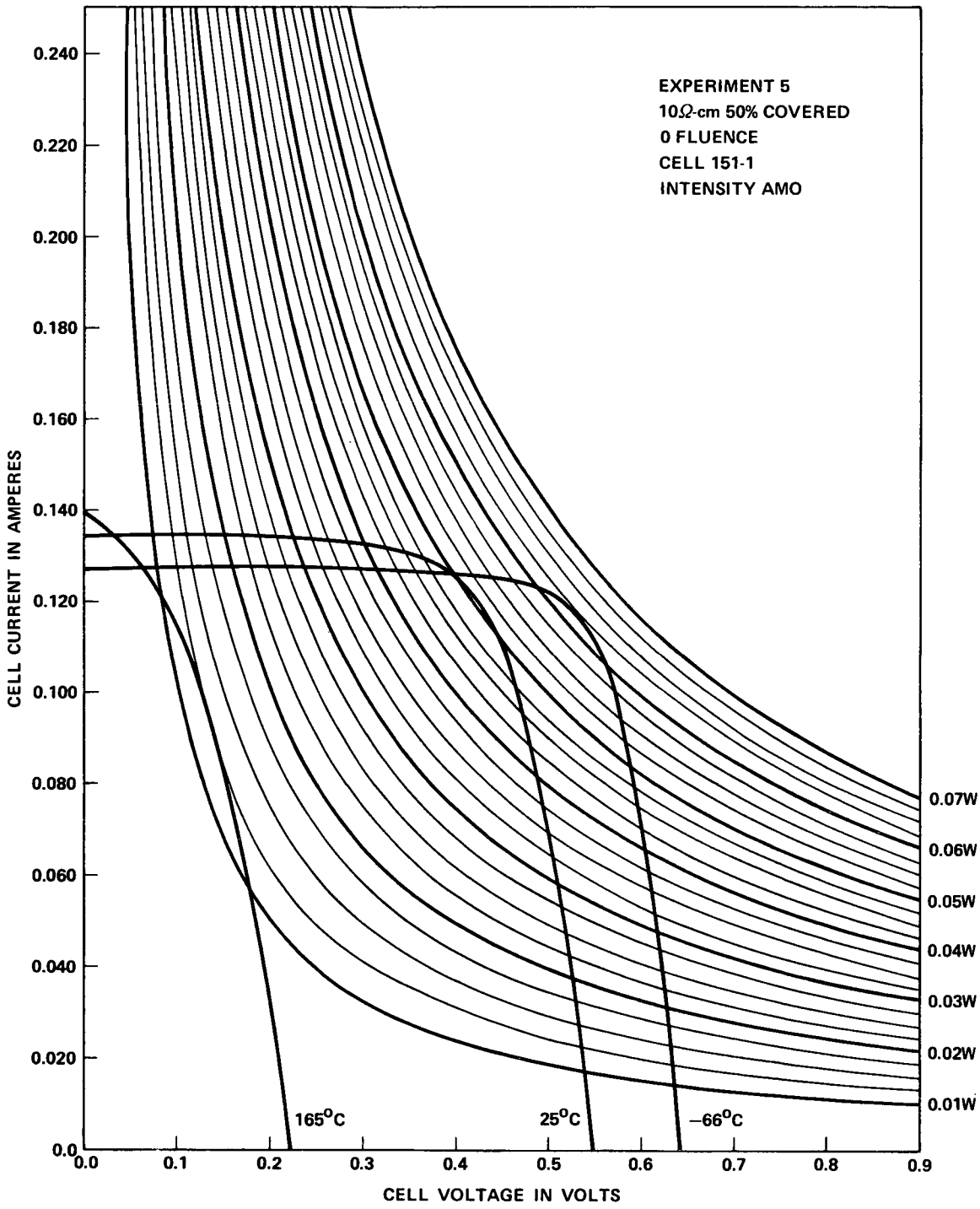
EXPERIMENT 5
10Ω-cm 50% COVERED
0 FLUENCE
CELL 151-1
INTENSITY AMO
CELL CURRENT IN AMPERES
CELL VOLTAGE IN VOLTS
0.240
0.220
0.200
0.180
0.160
0.140
0.120
0.100
0.080
0.060
0.040
0.020
0.0
0.0
0.1
0.2
0.3
0.4
0.5
0.6
0.7
0.8
0.9
0.07W
0.06W
0.05W
0.04W
0.03W
0.02W
0.01W
165°C
25°C
−66°C

Figure 14

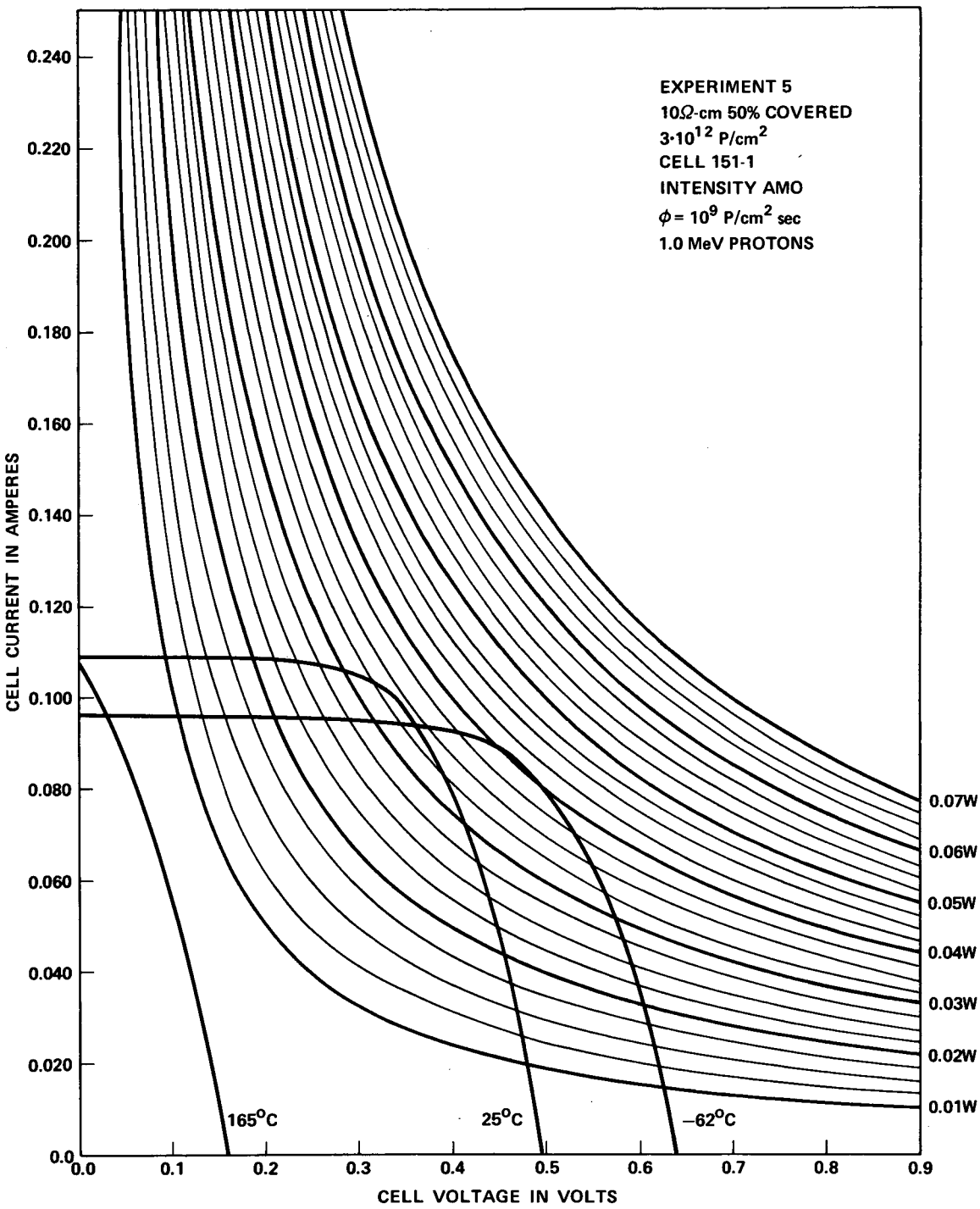
EXPERIMENT 5
10Ω-cm 50% COVERED
3·10^12 P/cm^2
CELL 151-1
INTENSITY AMO
φ = 10^9 P/cm^2 sec
1.0 MeV PROTONS
CELL CURRENT IN AMPERES
0.240
0.220
0.200
0.180
0.160
0.140
0.120
0.100
0.080
0.060
0.040
0.020
0.0
0.07W
0.06W
0.05W
0.04W
0.03W
0.02W
0.01W
165°C
25°C
−62°C
0.0
0.1
0.2
0.3
0.4
0.5
0.6
0.7
0.8
0.9
CELL VOLTAGE IN VOLTS

Figure 15

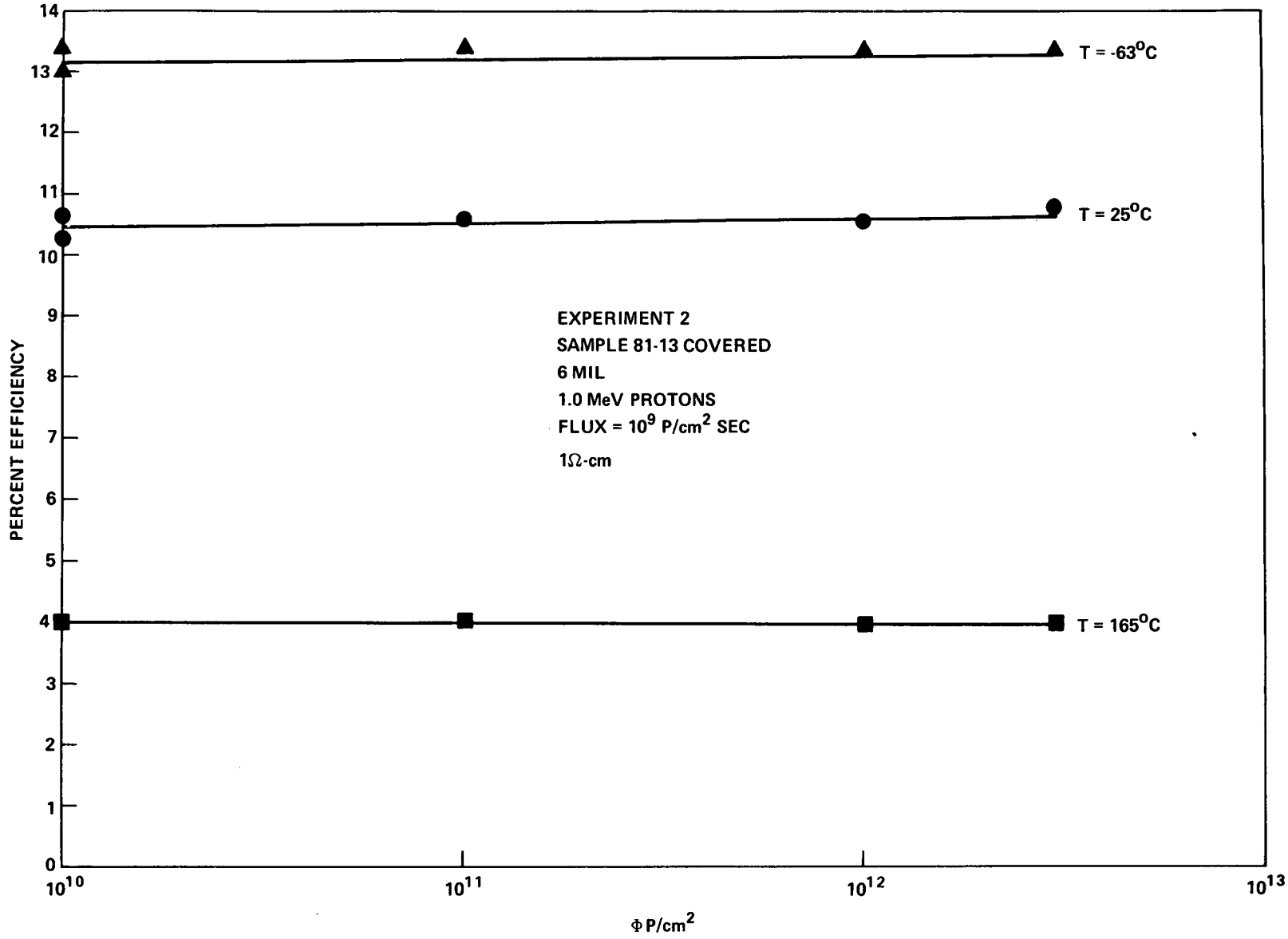
PERCENT EFFICIENCY
14
13
12
11
10
9
8
7
6
5
4
3
2
1
0
10^{10}
10^{11}
10^{12}
10^{13}
Φ P/cm^2
T = -63°C
T = 25°C
T = 165°C
EXPERIMENT 2
SAMPLE 81-13 COVERED
6 MIL
1.0 MeV PROTONS
FLUX = 10^9 P/cm^2 SEC
1Ω-cm

Figure 16

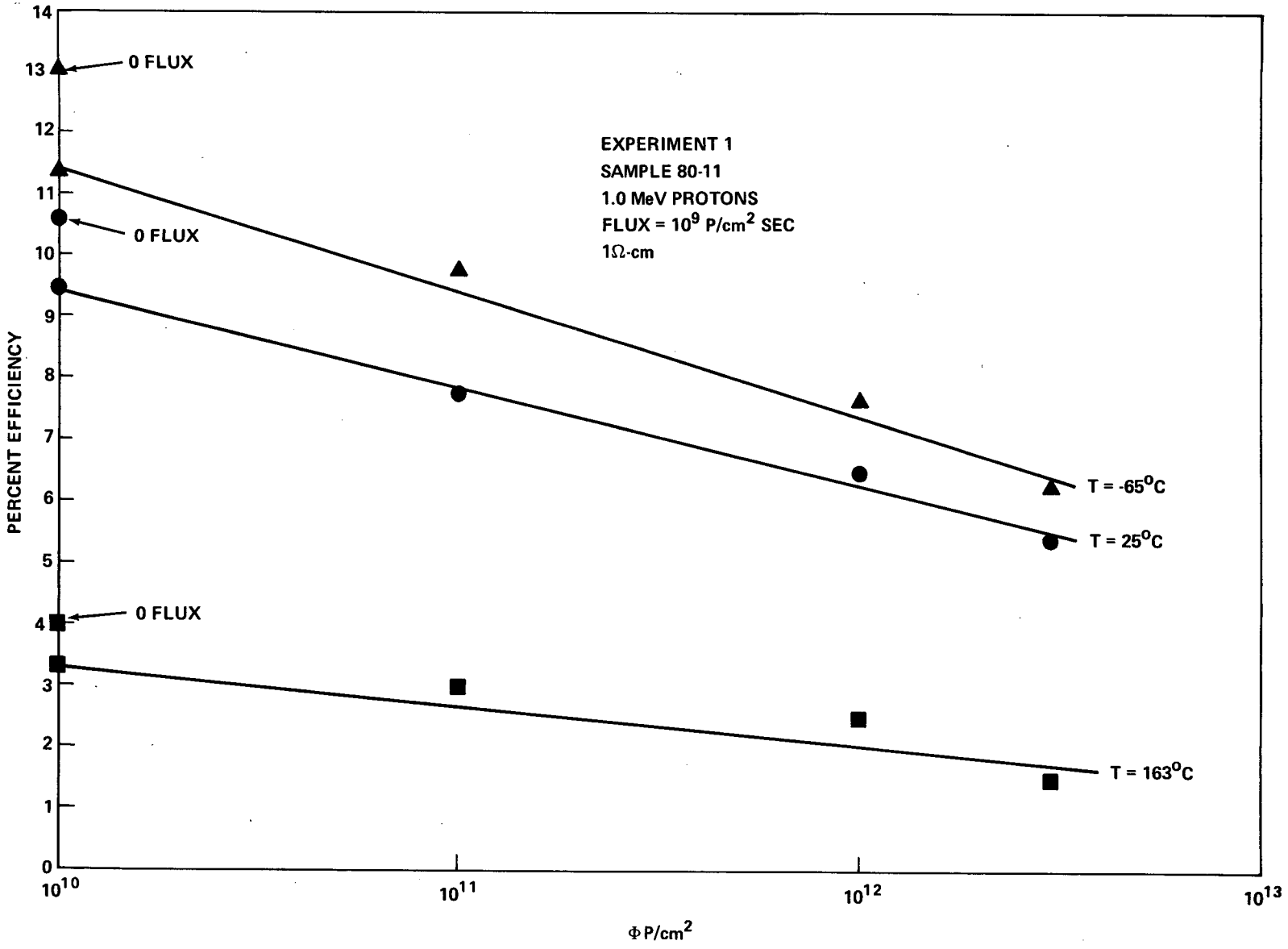
EXPERIMENT 1
SAMPLE 80-11
1.0 MeV PROTONS
FLUX = 10^9 P/cm^2 SEC
1Ω-cm
0 FLUX
0 FLUX
0 FLUX
T = -65°C
T = 25°C
T = 163°C
PERCENT EFFICIENCY
0
1
2
3
4
5
6
7
8
9
10
11
12
13
14
10^{10}
10^{11}
10^{12}
10^{13}
Φ P/cm^2

Figure 17

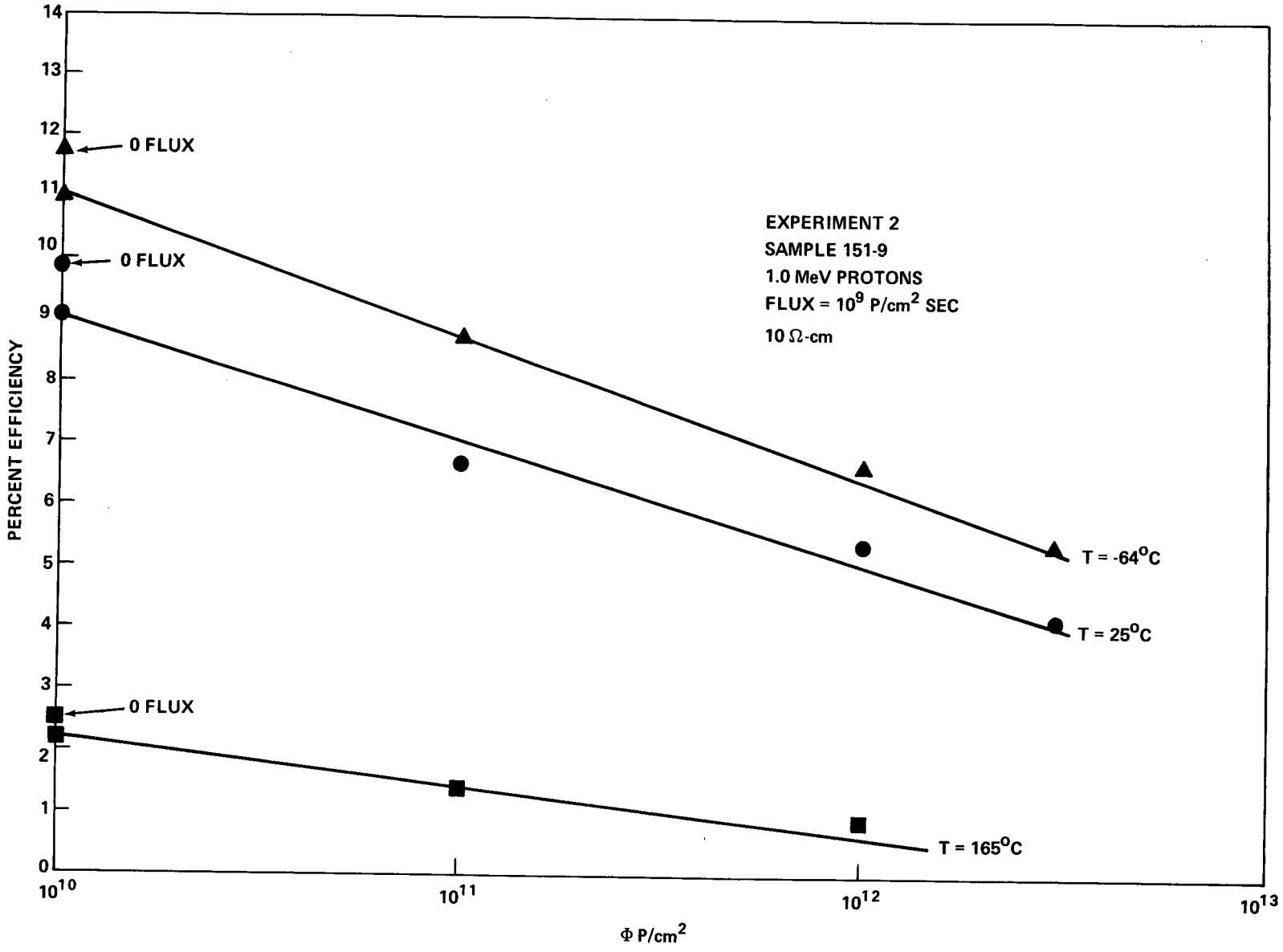
14
13
12
11
10
9
8
7
6
5
4
3
2
1
0
PERCENT EFFICIENCY
0 FLUX
0 FLUX
0 FLUX
EXPERIMENT 2
SAMPLE 151-9
1.0 MeV PROTONS
FLUX = 10^9 P/cm^2 SEC
10 Ω-cm
T = -64°C
T = 25°C
T = 165°C
10^10
10^11
10^12
10^13
Φ P/cm^2

Figure 18

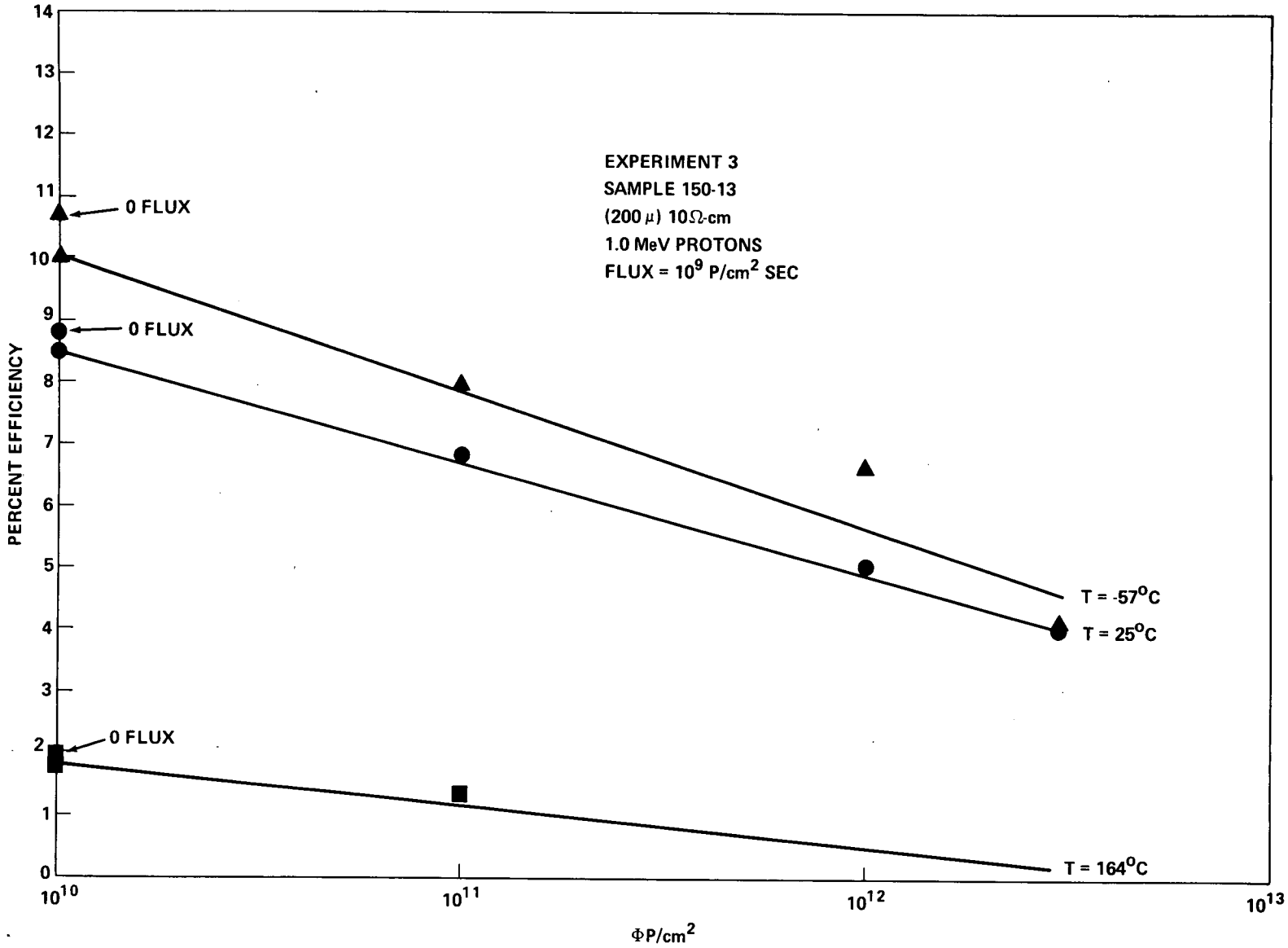
EXPERIMENT 3
SAMPLE 150-13
(200 μ) 10Ω-cm
1.0 MeV PROTONS
FLUX = 10^9 P/cm^2 SEC
0 FLUX
0 FLUX
0 FLUX
T = -57°C
T = 25°C
T = 164°C
PERCENT EFFICIENCY
ΦP/cm^2
0
1
2
3
4
5
6
7
8
9
10
11
12
13
14
10^10
10^11
10^12
10^13

Figure 19

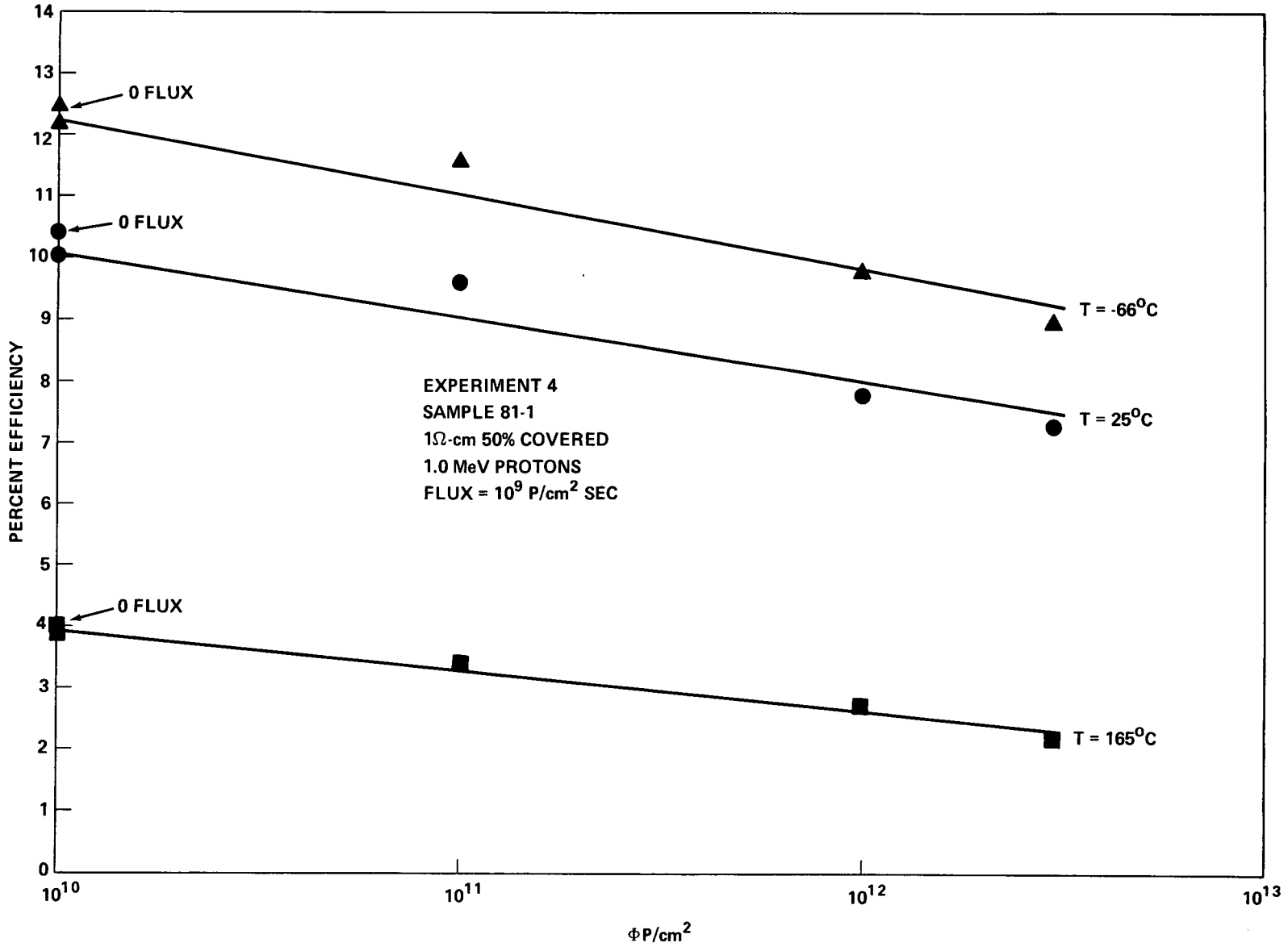
14
13
12
11
10
9
8
7
6
5
4
3
2
1
0
PERCENT EFFICIENCY
0 FLUX
0 FLUX
0 FLUX
T = -66°C
T = 25°C
T = 165°C
EXPERIMENT 4
SAMPLE 81-1
1Ω-cm 50% COVERED
1.0 MeV PROTONS
FLUX = 10^9 P/cm^2 SEC
10^10
10^11
10^12
10^13
ΦP/cm^2

Figure 20

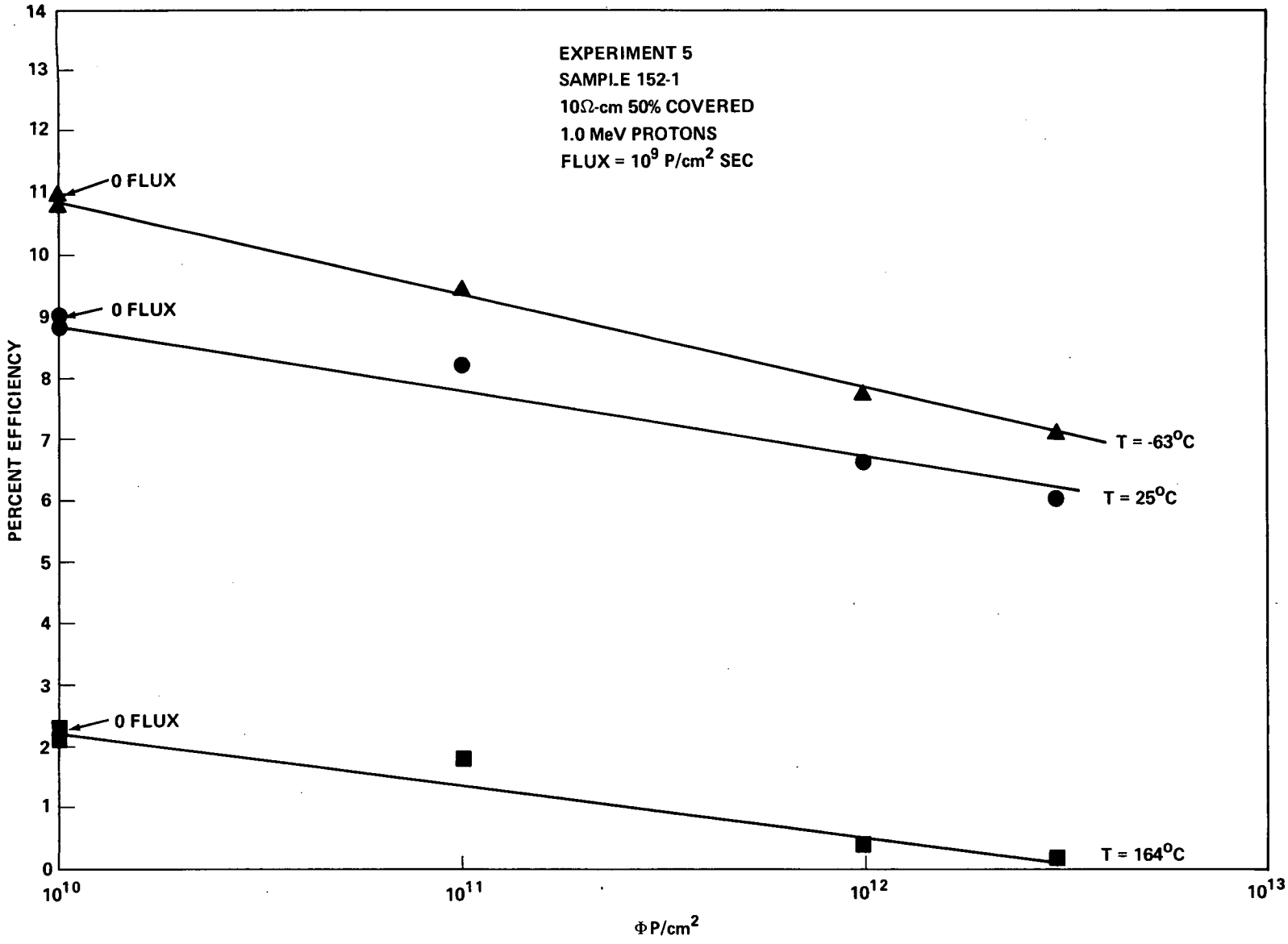
EXPERIMENT 5
SAMPLE 152-1
10Ω-cm 50% COVERED
1.0 MeV PROTONS
FLUX = 10^9 P/cm^2 SEC
0 FLUX
0 FLUX
0 FLUX
T = -63°C
T = 25°C
T = 164°C
PERCENT EFFICIENCY
ΦP/cm^2
10^{10}
10^{11}
10^{12}
10^{13}
0
1
2
3
4
5
6
7
8
9
10
11
12
13
14

Figure 21

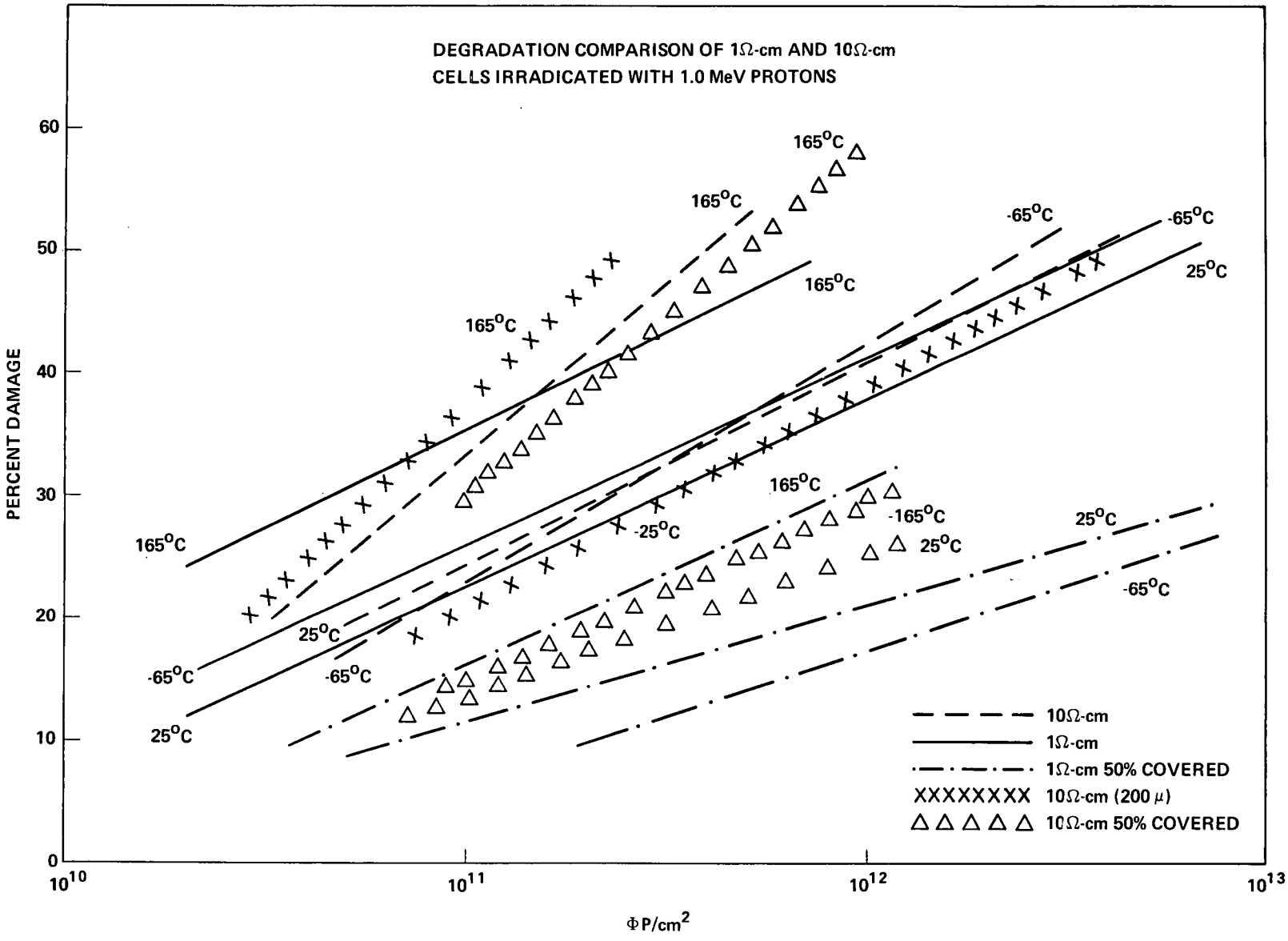
DEGRADATION COMPARISON OF 1Ω-cm AND 10Ω-cm
CELLS IRRADICATED WITH 1.0 MeV PROTONS
PERCENT DAMAGE
ΦP/cm²
0
10
20
30
40
50
60
10¹⁰
10¹¹
10¹²
10¹³
165°C
-65°C
25°C
-25°C
-165°C
10Ω-cm
1Ω-cm
1Ω-cm 50% COVERED
10Ω-cm (200 μ)
10Ω-cm 50% COVERED

Figure 22

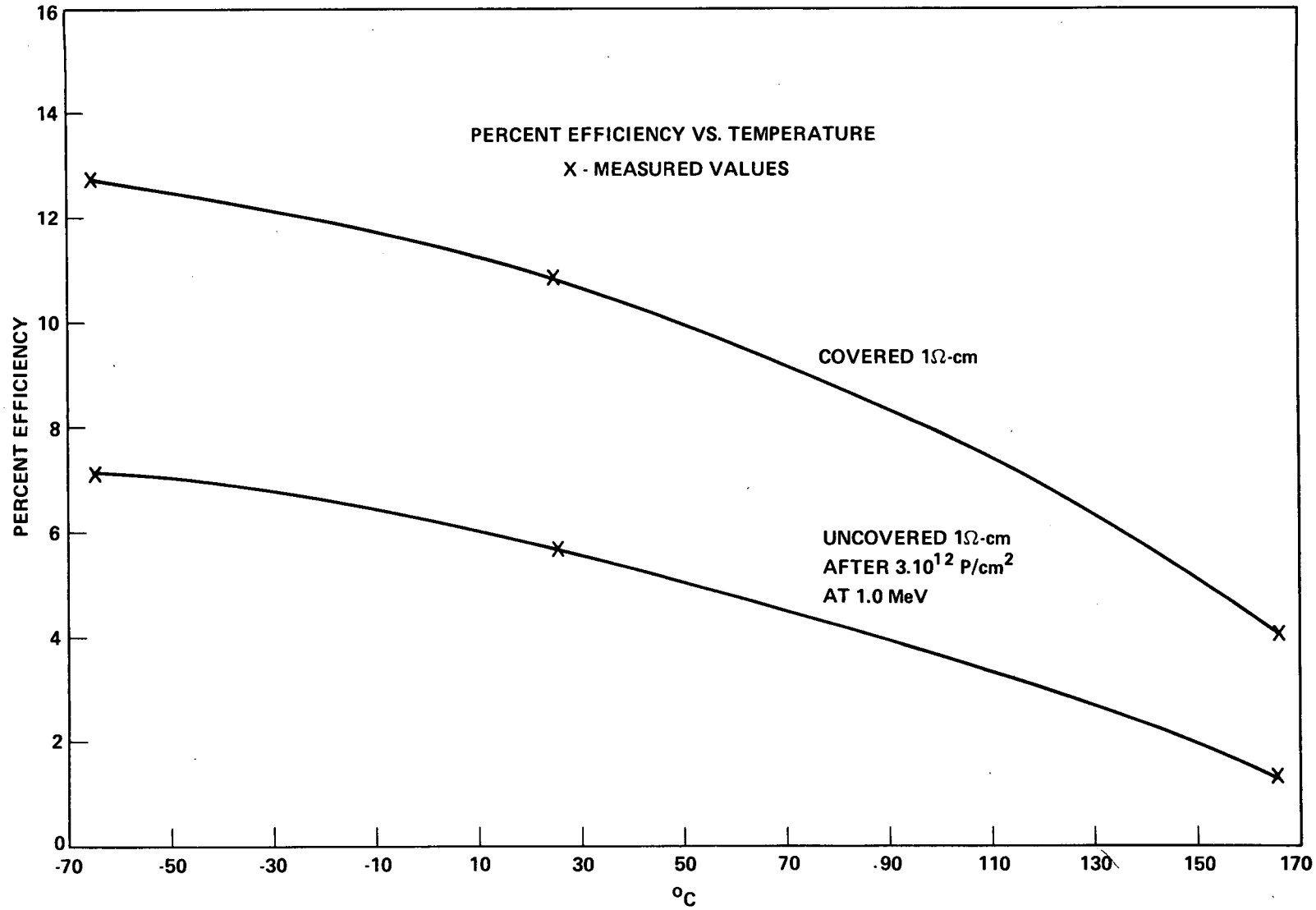

Figure 23

☆ U.S. GOVERNMENT PRINTING OFFICE: 1972—735-966/469